Catalyst Design Insights from Modelling a Titanium-Catalyzed Multicomponent Reaction

Kelly E. Aldrich, Dhwani Kansal, and Aaron L. Odom*

Michigan State University, Department of Chemistry, 578 S. Shaw Ln, East Lansing, MI 48824

odom@chemistry.msu.edu

Table of Contents

Syntheses of Titanium Complexes

Synthesis of Ti(OPh$^{2,4\text{-di-t-butyl}}$)$_4$ (**6e**) can be found in the manuscript. The syntheses and characterization data for the other derivatives are below.

*Synthesis of Ti(OPh$^{2\text{-t-butyl-4-methyl}}$)$_4$ (**6b**)*

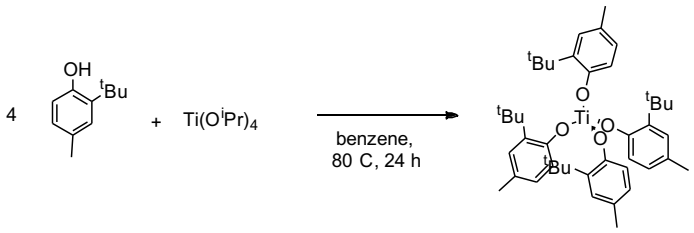

In a glovebox, a Schlenk flask was charged with 70 mL benzene, Ti(O^{i}Pr)$_4$ (1.09 g, 3.84 mmol), and a stir bar. To this solution was added 2-tert-butyl-4-methylphenol (2.53 g, 15.4 mmol, 4 equiv). The flask was sealed and transferred to a Schlenk line, where it was attached to a reflux condenser under N_2. The solution was refluxed for 24 h. The volatiles were removed in vacuo to provide a bright yellow residue. The flask was transferred back to the glovebox where the yellow solids were recrystallized from pentanes to provide pure **6b (**2.16 g, 87%). X-ray quality single crystals were grown from a concentrated solution in *n*-hexane at –35 °C. ^{1}H NMR (500 MHz, benzene-d_6): 7.35 (d, J = 8.0 Hz, 4H), 7.11 (d, J = 2.2 Hz, 4H), 6.72 (dd, J = 8.2, 2.1 Hz, 4H), 2.09 (s, 12H), 1.56 (s, 36H).^{13}C NMR (126 MHz, chloroform-*d*): 161.80, 136.30, 131.70, 127.66, 127.17, 122.86, 34.85, 30.23, 21.20. Elemental Analysis calc. for $TiC_{44}H_{60}O_4$: C, 75.41; H, 8.63; N, 0. Found: C, 74.93; H, 8.89; N, 0.10.

*Synthesis of Ti(OPh$^{2\text{-t-butyl-4-Br}}$)$_4$ (**6f**)*

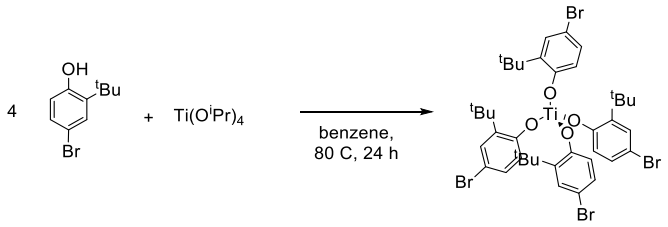

The procedure provided for the preparation of **6b** was followed to prepare **6f** using Ti(O^{i}Pr)$_4$ (0.568 g, 2 mmol), 2-*tert*-butyl-4-bromophenol (1.83 g, 8 mmol), and benzene (70 mL). The product was recrystallized from pentanes at –35 °C to yield pure **6f** (1.42 g, 74%). X-ray quality crystals were grown from pentanes at –35 °C. ^{1}H NMR (500 MHz, benzene-d_6) 7.37 (d, J = 2.5 Hz, 4H), 7.17 (dd, J = 8.5, 2.4 Hz, 4H), 6.86 (d, J = 8.5 Hz, 4H), 1.37 (s, 36H). ^{13}C NMR (126 MHz, benzene-d_6) 162.52, 138.85, 130.26, 130.20, 124.12, 116.13, 34.70, 29.42, 28.89. Elemental Analysis calc. for $TiC_{40}H_{48}O_4Br_4$: C, 50.04; H, 5.04; N, 0. Found: C, 49.49; H, 4.58; N, 0.09.

*Synthesis of Ti(OPh$^{2\text{-t-butyl-4-F}}$)$_4$ (**6d**)*

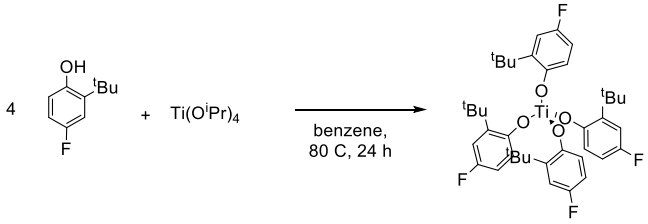

The procedure provided for the preparation of **6b** was followed to prepare **6d** using Ti(O^{i}Pr)$_4$ (888 μL, 3 mmol), 2-*tert*-butyl-4-fluorophenol (2.00 g, 12 mmol), and benzene (70 mL). The product was recrystallized from pentanes at –35 °C to yield pure **6d** (2.36g, 90%). X-ray quality crystals were grown from *n*-hexane at –35 °C. ^{1}H NMR (500 MHz, benzene-d_6): 7.06–7.01 (m, 4H), 6.96 (dt, J = 10.6, 2.3 Hz, 4H), 6.58–6.43 (m, 4H), 1.29 (d, J = 1.8 Hz, 36H).^{13}C NMR (126 MHz, benzene-d_6): 163.34–158.24 (m), 157.73, 139.02 (d), 123.69 (d), 114.27 (d), 113.77 (d), 35.11, 29.84.^{19}F NMR (470 MHz, benzene-d_6): –117.57 to –119.68 (m). Elemental Analysis calc. for $TiC_{40}H_{48}O_4F_4$: C, 67.04; H, 6.75; N, 0. Found: C, 66.36; H, 6.87; N, 0.24.

*Synthesis of Ti(OPh$^{2\text{-t-butyl-4-methoxy}}$)$_4$ (**6a**)*

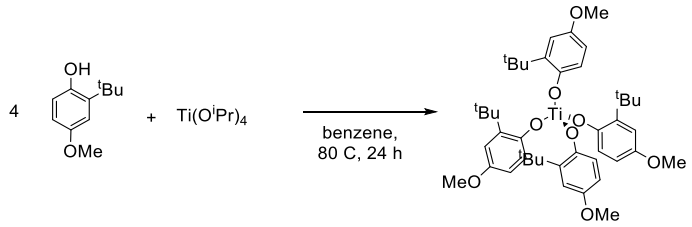

The procedure provided for the preparation of **6b** was followed to prepare **6a** using Ti(O^{i}Pr)$_4$ (1.09 g, 3.83 mmol), 2-*tert*-butyl-4-methoxyphenol (2.77 g, 15.4 mmol), and benzene (70 mL). The product was recrystallized from pentanes at –35 °C to yield pure **6a** (2.21 g, 80%).^{1}H NMR (500 MHz, benzene-d_6): 7.37 (dd, J = 8.6, 1.1 Hz, 4H), 7.04 (dd, J = 3.1, 1.1 Hz, 4H), 6.57–6.35 (m, 4H), 3.30 (s, 12H), 1.55 (d, J = 1.2 Hz, 36H). ^{13}C NMR (126 MHz, benzene-d_6): 158.50, 155.07, 137.82, 123.22, 113.52, 110.67, 54.66, 34.87, 29.86. Elemental Analysis calc. for $TiC_{44}H_{60}O_8$: C, 69.05; H, 7.86; N, 0. Found: C, 69.10; H, 7.91; N, 0.09.

*Synthesis of Ti(OPh$^{2\text{-t-butyl-4-trifluoromethyl}}$)$_4$ (**6g**)*

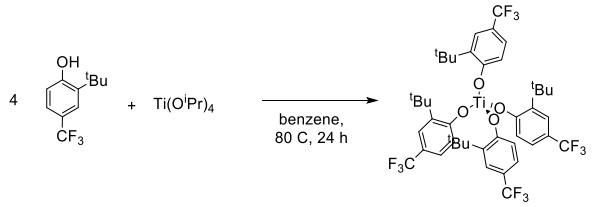

The procedure provided for the preparation of **6b** was followed to prepare **6g** using Ti(O^{i}Pr)$_4$ (340 µL, 1.12 mmol), 2-*tert*-butyl-4-trifluoromethylphenol (0.973 g, 4.46 mmol), and benzene (70 mL). The product was recrystallized from a 1:1 mixture of Et_2O and pentanes at –35 °C to yield pure **6g** (670 mg, 70%). X-ray quality crystals were grown from *n*-hexane at –35 °C. ^{1}H NMR (500 MHz, benzene-d_6): 7.69 (d, J = 2.2 Hz, 4H), 7.13 (d, J = 2.2 Hz, 4H), 7.08 (d, J = 8.3 Hz, 4H), 1.27 (s, 36H). ^{13}C NMR (126 MHz, benzene-d_6): 165.20, 137.67, 125.65 (d), 124.91 (q), 124.67 (d), 122.76, 116.21, 34.71, 29.32. ^{19}F NMR (470 MHz, benzene-d_6): –61.45. Elemental Analysis calc. for $TiC_{44}H_{48}F_{12}O_4$: C, 57.65; H, 5.28; N, 0. Found: C, 57.37; H, 5.41; N, 0.18.

*Synthesis of Ti(OPh$^{2\text{-t-butyl}}$)$_4$ (**6c**)*

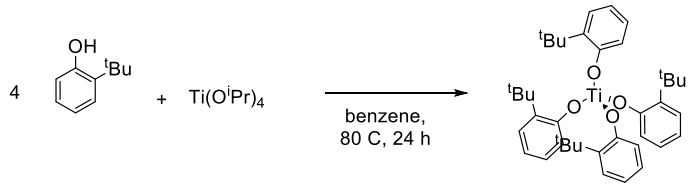

The procedure provided for the preparation of **6b** was followed to prepare **6c** using Ti(O^{i}Pr)$_4$ (383 μL, 1 mmol), 2-*tert*-butylphenol (0.601 g, 4 mmol), and benzene (30 mL). The product was recrystallized from a 1:1 mixture of Et_2O and pentanes at –35 °C to yield **6c** (389 mg, 60%). X-ray quality crystals were grown from a concentrated solution of the complex in toluene layered with *n*-hexane at –35 °C. ^{1}H NMR (500 MHz, benzene-d_6): 7.38 (dd, J = 7.9, 1.2 Hz, 4H), 7.20 (dd, J = 7.9, 1.7 Hz, 4H), 6.91 (td, J = 7.6, 1.7 Hz, 4H), 6.84–6.73 (m, 4H), 1.49 (s, 36H). ^{13}C NMR (126 MHz, benzene-d_6): 163.70, 136.52, 127.38, 126.77, 122.97, 122.86, 34.68, 29.96. Elemental Analysis calc. for$TiC_{40}H_{52}O_4$: C, 74.52; H, 8.13; N, 0. Found: C, 75.06; H, 8.36; N, 0.17.

Synthesis of Chromium Complexes

The starting material NCr(N^{i}Pr$_2$)$_3$ was prepared using the literature procedure.[1] Substituted phenols were purchased from Sigma-Aldrich and were purified by sublimation prior to use.

Synthesis of NCr(N^{i}Pr$_2$)$_2$(OPh$^{4\text{-methyl}}$): A scintillation vial was charged with NCr(N^{i}Pr$_2$)$_3$ (50 mg, 0.14 mmol), a stir bar, and Et_2O (3 mL). The vial was chilled in a cold well with liquid nitrogen until the Et_2O solution was almost frozen. The chilled solution was stirred, and a solution of HOPh$^{4\text{-methyl}}$ (15 mg, 0.14 mmol) in Et_2O was added dropwise. The solution went from beet-colored to red upon addition. The solution was warmed to room temperature and stirred for 2 h. The volatiles were removed in vacuo yielding a dark red residue. The residue was dissolved in a minimum amount of *n*-hexane, filtered through Celite, and chilled to –35 °C to yield crystals of NCr(N^{i}Pr$_2$)$_2$(OPh$^{4\text{-methyl}}$) (27 mg, 52%). ^{1}H NMR (500 MHz, chloroform-*d*): 6.97 (d, J = 7.8 Hz, 2H), 6.88 (d, J = 7.8 Hz, 2H), 5.02 (s, 2H), 3.73 (s, 2H), 2.24 (s, 3H), 1.83 (d, J = 6.3 Hz, 6H), 1.56–1.39 (m, 6H), 1.28–0.95 (m, 13H). ^{13}C NMR (126 MHz, chloroform-*d*)

129.37, 128.29, 117.15, 58.26, 55.22, 30.45, 30.13, 21.42, 21.11, 20.78. Elemental Analysis calc. for $CrC_{19}H_{35}ON_3$: C, 61.10; H, 9.45; N, 11.25. Found: C, 61.47; H, 10.06; N, 11.42.

Synthesis of $NCr(N^iPr_2)_2(OPh^{4\text{-bromo}})$: A scintillation vial was charged with $NCr(N^iPr_2)_3$ (50 mg, 0.14 mmol), a stir bar, and Et_2O (3 mL). The vial was chilled in a cold well with liquid nitrogen until the Et_2O solution was almost frozen. The chilled solution was stirred and a solution of $HOPh^{4\text{-bromo}}$ (24 mg, 0.14 mmol) in Et_2O was added dropwise. The solution went from beet-colored to red upon addition. The solution was warmed to room temperature and stirred for 2 h. The volatiles were removed in vacuo yielding a dark red residue. The residue was dissolved in a minimal amount of toluene and was filtered through Celite. The filtrate was collected and layered with *n*-hexane. The layered solution was chilled to –35 °C for 1 week to yield crystals of $NCr(N^iPr_2)_2(OPh^{4\text{-bromo}})$ (38 mg, 62%). ^{1}H NMR (500 MHz, chloroform-*d*): 7.23–7.12 (m, 2H), 6.90–6.74 (m, 2H), 5.04 (septet, J = 6.5 Hz, 2H), 3.75 (septet, J = 6.4 Hz, 2H), 1.85 (d, J = 6.2 Hz, 6H), 1.46 (d, J = 6.3 Hz, 6H), 1.15 (d, J = 6.4 Hz, 12H). ^{13}C NMR (126 MHz, chloroform-*d*): 165.93, 131.60, 119.56, 110.65, 58.46, 55.59, 30.50, 30.24, 21.48, 21.20. Elemental Analysis calc. for $CrC_{18}H_{32}ON_3Br$: C, 49.32; H, 7.36; N, 9.59. Found: C, 49.09; H, 7.41; N, 9.33.

Catalytic Product Synthesis and Isolation

Synthesis of Iminoamination Product from aniline, 1-octyne, and ^{t}*BuNC*

A 15 mL pressure tube was charged with $Ti(dpm)(NMe_2)_2$ (62 mg), toluene (1 mL), and a stir bar. To the stirred solution was added a 1 mL solution containing aniline (186 mg, 2 mmol, 1 equiv) in toluene. This mixture was stirred for 10 min at room temperature over which time the solution went from transparent bright orange to an opaque reddish-brown. Then a 1 mL solution containing ^{t}BuNC (184 mg, 2 mmol, 1 equiv) and 1-octyne (220 mg, 2 mmol, 1 equiv) in toluene was added to the solution in the pressure tube. The tube was sealed and transferred from the glovebox to a 110 °C oil bath. The tube was heated and stirred for 24 h. The tube was removed from the bath and allowed to ambiently cool. The volatiles were removed by rotary evaporation, and the resulting crude, dark brown oil was separated by column chromatography (Al_2O_3, hexanes with 1% TEA and gradient Et_2O from 0 to 30%). The isolated product was obtained as an

orange oil (310 mg, 54%), which proved to be a mixture of regioisomers (Table 1). ^{1}H NMR (500 MHz, chloroform-*d*): (**A**) 9.97 (s, 1H), 4.72 (d, *J* = 8.0 Hz, 1H), 1.27 (s, 9H), 0.90 (m, 3H); (**B**) 10.83 (s, 1H), 7.77 (d, *J* = 2.8 Hz, 1H), 7.11 (d, *J* = 2.8 Hz, 1H), 1.32 (s, 9H), 0.84 (t, 3H); (**A/B**) 7.33–7.26 (m, 4H), 7.04 (d, *J* = 7.7 Hz, 2H), 7.03–6.97 (m, 1H), 6.85–6.78 (m, 3H), 2.37 (s, 1H), 2.22–2.09 (m, 3H), 1.48 (m, 5H), 1.18 (m, 8H).^{13}C NMR (126 MHz, chloroform-*d*): 171.01, 153.80, 151.55, 150.11, 146.87, 142.28, 129.06, 128.43, 122.66, 121.83, 121.38, 119.00, 103.60, 91.79, 52.60, 51.03, 33.68, 33.21, 32.91, 31.93, 31.80, 31.46, 30.36 (d, *J* = 1.9 Hz), 30.31, 29.47, 29.32, 28.74, 28.67, 27.73, 23.69, 22.72, 22.47, 14.15, 14.05. High-Resolution MS: QTOF EI (positive ion) calc. for $C_{19}H_{31}N_2$: 287.2487; found: 287.2484. Elemental Analysis calc. for $C_{19}H_{30}N_2$: C, 79.66; H, 10.56; N, 9.78. Found: C, 79.88; H, 10.44; N, 9.44.

Synthesis of 2,3-diaminopyrrole from aniline, 1-octyne, and 2 ^{t}BuNC

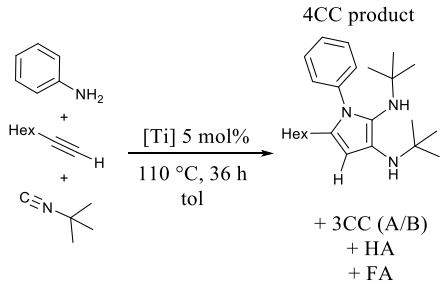

On several occasions, the product mass that corresponds to the coupling of 1 equiv aniline, 1 equiv alkyne, and 2 equiv of isonitrile (4-component coupling, 4CC) was observed by GC/MS in reactions catalyzed by homogeneous titanium catalysts.[2] Typically, the amount of this product was relatively small. However, under certain conditions when reactions were carried out on large enough scales, substantial masses of the 4CC product were noted in various column fractions when isolating the iminoamination products by column chromatography. On one such occasion, a very clean fraction of the 4CC product was isolated from a 2 mmol scale reaction (H_2NPh, ^{t}BuNC, 1-octyne) with 5 mol% Ti(dpm)(NMe_2)$_2$ as precatalyst. The 4CC product was the first compound eluted from an alumina column (93 mg, 0.25 mmol, 13% relative to 2 mmol H_2NPh as limiting reagent), basified with 1% TEA in hexane. Note, from the same column, the

iminoamination product was also isolated, but as a later fraction with the addition of Et_2O on a gradient from 0-30%.

The 4CC product was characterized by GCMS, HRMS, ^{1}H NMR, ^{13}C NMR, and a few additional 2D NMR techniques. The above structural assignment seems to most closely match the characterization data for this product, in agreement with previous studies by our group.[2] ^{1}H NMR (500 MHz, benzene-d_6): 7.43 (d, J = 7.1 Hz, 2H), 7.13 (t, J = 7.8 Hz, 2H), 6.97 (t, J = 7.5 Hz, 1H), 6.53 (t, J = 0.9 Hz, 1H), 2.99 (s, 1H), 2.68–2.54 (m, 2H), 2.34 (s, 1H), 1.75 (pentet, J = 7.7 Hz, 2H), 1.52–1.42 (m, 3H), 1.40–1.29 (m, 06H), 1.23 (s, 12H), 0.92 (s, 15H). ^{13}C NMR (126 MHz, benzene-d_6): 142.18, 128.80, 125.41, 125.16, 123.74, 122.06, 121.84, 113.63, 55.46, 54.53, 32.33, 30.66, 30.60, 30.54, 30.07, 26.37, 23.16, 14.41. HRMS: QTOF EI (positive ion) calc. for $C_{24}H_{40}N_3^+$: 370.3222; found: 370.3218. Elemental analysis calc. for $C_{24}H_{39}N_3$: C, 77.99; H, 10.69; N, 11.37. Found: C, 78.09; H, 10.85; N, 11.11.

In Situ Investigations of Titanium Complex Nuclearity—DOSY Molecular Weight Determinations in C_6D_6

Note that D represents the diffusion coefficient, which is given in units of $1*10^{-4}$ m^2/s.

Solution Molecular Weight of {Ti(OArCH$_2$ArO)(μ-Ntolyl)}$_2$·HNMe$_2$

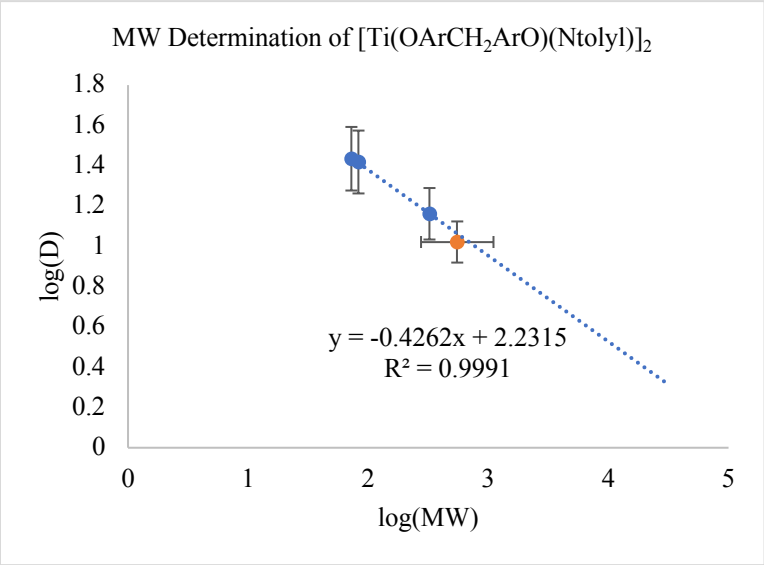

Compound	MW (g/mol)	Log(MW)	D	Log(D)	Error in Diffusion Coefficient
THF	72	1.86	27.2	1.45	0.86
Benzene	83	1.92	26.2	1.41	0.74
TMS_4Si	321	2.51	14.5	1.12	1.03
Expt weight for {Ti(Ntolyl)(bisphenoxide)}$_x$	551 (± 62)	2.74	10.5	1.02	0.82
Calc'd Dimer Weight	983				
Calc'd Monomer Weight	492 (w/HNMe$_2$ =537)				

Solution Molecular Weight of Ti(OArCH$_2$ArO)I$_2$

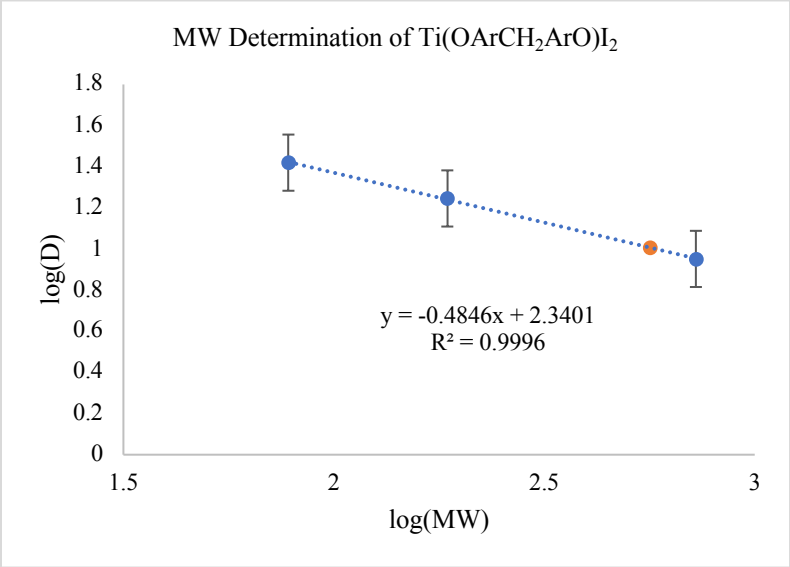

Compound	MW	log(MW)	D	log(D)	Error in Diffusion Coefficient
Fc	186.04	2.27	17.61	1.25	0.25
C_6D_5H	78	1.89	26.29	1.42	0.58
Ti(OArArO)$_2$	724.85	2.86	8.95	0.95	0.81
Experimental Weight Ti(OArARrO)(I)$_2$	563 ± 94	2.75	10.16	1.01	0.20
Calc Monomer Weight	638				

Solution Molecular Weight of Ti(OArCH$_2$ArO)(O^{i}Pr)$_2$

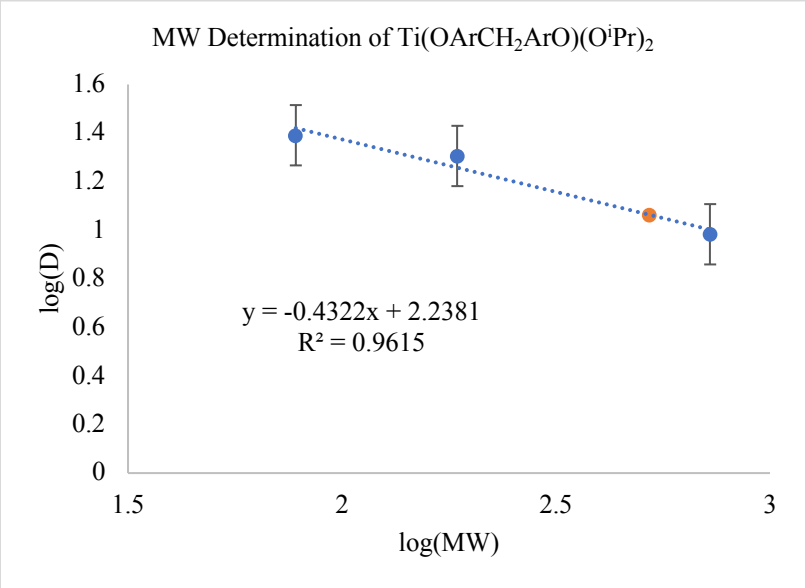

Compound	MW	log(MW)	D	log (D)	Error in Diffusion Coefficient
Fc	186.04	2.269606	20.21	1.305566	0.76
C_6D_5H	78	1.892095	24.6	1.390935	0.76
Ti(OArCH$_2$ArO)$_2$	724.85	2.860248	9.62	0.983175	1.4
Exper. Weight Ti(OArCH$_2$ArO)(O^{i}Pr)$_2$	523 ± 74	2.718186	11.57	1.063333	0.33
Calc. Monomer Weight	504				

*Solution Molecular Weight of {Ti(dpm)(μ-Ntolyl)}$_2$ (**2^{tol}**)*

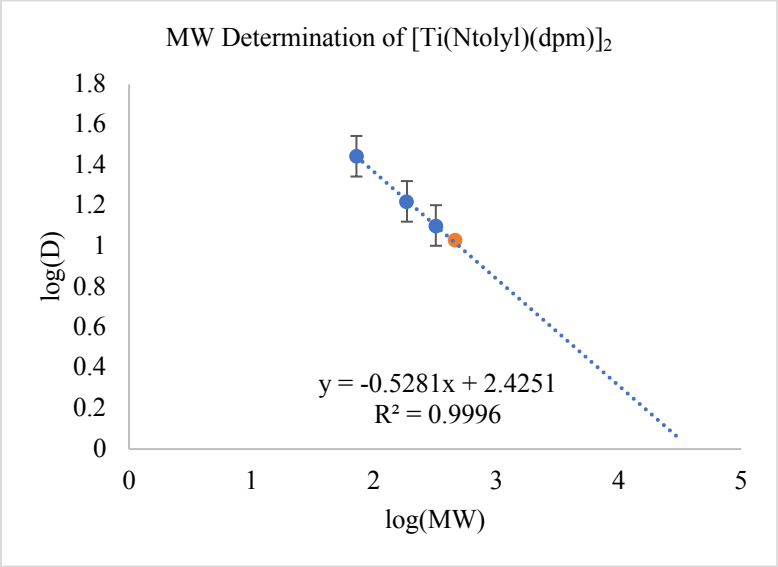

Compound	MW (g/mol)	Log(MW)	D	log(D)	Error in Diffusion Coeffcient
benzene	72	1.86	27.9	1.45	0.33
Fc	186	2.27	16.7	1.22	0.14
TMS_4Si	321	2.51	12.7	1.10	0.32
Exper. Weight $\{Ti(dpm)(Ntolyl)\}_n$	465 ± 51	2.67	10.8	1.03	0.13
Calc. Monomer Weight	325				
Calc. Dimer Weight	651				

Iminoamination Experiments

The following reagents were measured separately by mass: (1) Ti(dpm)(NMe_2)$_2$ (**1**) (78-312 mg, 5-20 mol %), (2) dodecane (212 mg, 1.25 mmol, 0.05 M), (3) H_2NPh (465 mg-2.32 g, 5-25 mmol), (4) ^{t}BuNC (415-830 mg, 5-10 mmol), and (5) 1-octyne (550 mg-2.75 g, 5-25 mmol). In a scintillation vial, the Ti(dpm)(NMe_2)$_2$ (**1**) was dissolved in 5 mL toluene and the dodecane and H_2NPh were added, causing the solution to change colors from bright orange to dark reddish-brown. This solution was stirred at room temperature for 5-10 min and transferred to a 25.0 mL volumetric flask. The ^{t}BuNC and 1-octyne were added to the flask, and the solution was diluted to 25.0 mL with toluene. This solution was thoroughly mixed and transferred in 1 mL aliquots to sample tubes (generally 10-12 per entry). The tubes were sealed and transferred from the glovebox to a preheated oil bath. The elapsed time from the start of the reaction was recorded each time a sample was removed for GC analysis, ranging from 30 min to 28 h.

The samples were analyzed by GC-MS to look for reaction products and provide detection of unwanted side products. GC-FID was used to quantify the amounts of iminoamination product, hydroamination product, formamidine, and 4-component coupling product (2,3-diaminopyrrole) production in each sample based on external calibrations standardized with internal dodecane (0.05 M) from the authentic isolated products. The authentic samples had previously been obtained by separation from the organic reaction mixtures. The results of these experiments are shown in Table 1 in the manuscript.

Initial Rates of Catalysts 1 and 3

Experiments were done using 5 mol % (0.01 M) catalyst and 0.2 M 1-octyne, cyclohexylisonitrile, and aniline in toluene at 110 °C. The formation of product was followed relative to dodecane internal standard by GCFID. The initial rate vs time data are tabulated and plotted below. Reactions were followed to ~0.02 M (~10%) completion in product concentration. The fits in the plots below are forced through the origin, i.e., zero product at zero time (which was verified by examination of the reaction mixture prior to heating).

*$Ti(NMe_2)_2(dpm)$ (**1**)*

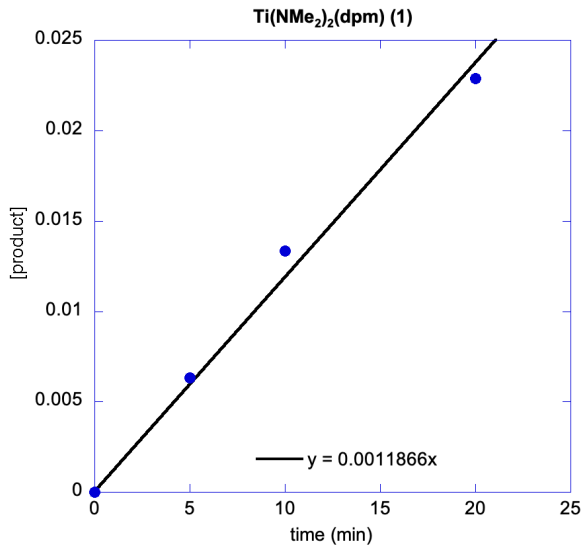

time (min)	[3CC] (M)
0	0
5	0.006337
10	0.013328
20	0.022899

*$Ti(NMe_2)_2(O_2Ar\text{-}6\text{-}CH_2)$ (**3**)*

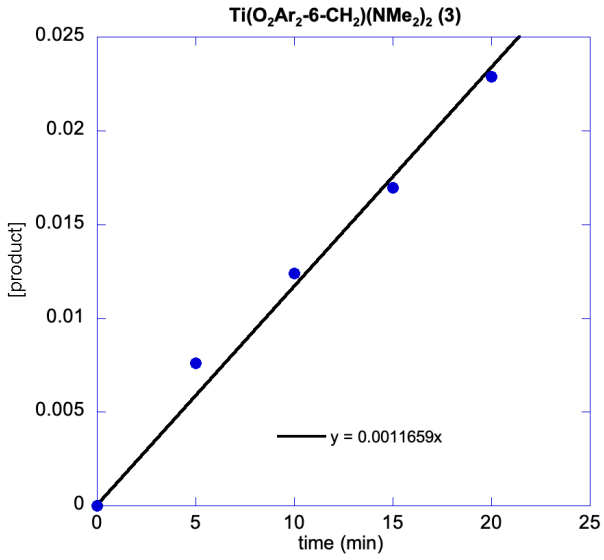

time (min)	[3CC] (M)
0	0
5	0.007612
10	0.012406
15	0.016954
20	0.02041

The slopes of the lines in the two initial rates experiments above are essentially identical, 0.0012 vs 0.0012 M/min. Consequently, the two catalysts **1** and **3** are judged to have identical rates under these conditions within error of the measurement.

LDP and $\%V_{bur}$ Measurements

Several of the LDP values utilized for the examination of ligand effects on the equilibrium distribution of ligand exchange products have been previously published (NMe_2, I, and O^iPr).[3] Other values have been re-established with improved accuracy to the NMR experiment protocol relative to the original values. The new values for these ligands are listed below. Preparation of the $NCr(N^iPr_2)_2X$ complexes generally followed literature procedures.[3-5]

Note that the LDP values used for the various 2-*tert*-butyl-4-R-phenoxide ligands are those obtained with the 4-R-phenoxide substituted derivatives on chromium. Previously, we have observed that inclusion of substitution in the 2-position of the phenoxide ligands imposes a steric interference on the LDP value obtained with the $NCr(N^iPr_2)_2X$ system. For example, when 2,4-dimethylphenoxide is examined by LDP, the value obtained is 11.98 kcal/mol. By comparison, the values for phenoxide and 4-methylphenoxide are 11.98 and 11.82 kcal/mol, respectively. This series highlights the steric effect of raising the LDP value when a substituent, such as those in the 2 or 6 positions of a phenoxide, encroach on the first coordination sphere of the metal. Subsequently, the LDP values listed below for the 2-*tert*-butyl-4-R-phenoxide ligands used with the $Ti(OAr)_4$ complexes are those determined from the $NCr(N^iPr_2)_2(OPh^{4\text{-}R})$ complexes.[6]

The $\%V_{bur}$ measurements for each ligand were determined from single crystal X-ray structures containing the ligand on 4-coordinate Ti. The exception to this was the O^iPr ligand, for which the $\%V_{bur}$ was determined using the dimeric crystal structure of $\{Ti(OArCH_2OAr)(O^iPr)(\mu\text{-}O^iPr)\}_2$. The O^iPr-ligands that interact with a single Ti metal were utilized for the size determination, rather than the bridging O^iPr-ligands in this structure. The $\%V_{bur}$ determined by this method was similar to previous determinations in the chromium-based LDP system. In fact, all $\%V_{bur}$ values for the X^- ligands determined here with titanium were very similar to previous determinations in the LDP system.

Equilibrium Data Modeling with Stereoelectronics

Ligand Sets where K_{eq} >> 2,000[a]		LDP (kcal/mol)	
A	**X**	NMe_2	9.34
NMe_2	Cl	O^iPr	10.56
O^iPr	Cl	Cl	14.97
OCy	Cl	Br	15.45
O^iPr	Br	pyrrolyl	13.64[c]
NMe_2	pyrrolyl in dpm	OCy	—[b]

[a]In these cases, literature reports demonstrate the formation of a single heteroleptic species from the combination of the homoleptic starting materials, TiA_4 and TiX_4. In other words, no observable disproportionation occurs. Using our model, we would estimate that K_{eq} involving these ligands would be >>K_{eq}, the experimental limit of our K_{eq} measurements. [b]Assumed to be the same as O^iPr electronically. [c]One could argue that a better estimate for the pyrrolyl in dpm would use 2-methylpyrrolyl, which has an LDP of 13.46 kcal/mol.

Ti(OArCH$_2$ArO)X$_2$		LDP	ΔLDP	(ΔLDP)^2	%V$_{bur}$	Δ%V$_{bur}$	(Δ%V$_{bur}$)^2	Expt. K_{eq}	Expt. Error	Model K_{eq}
A	NMe_2	9.34	-2.48	6.1504	21.9	0.7	0.49	1120	118	1136
	O^iPr[a]	10.33	-1.49	2.2201	17.4	-3.8	14.44	495	80	493
	I	15.8	3.98	15.8404	19.2	-2	4	1830	190	1716
	Cl	14.97	3.15	9.9225	16.8	-4.4	19.36	898	179	1010
A = 2-*tert*-butyl-4-Y-phenoxide where *Y is*	^{t}Bu	12.01	0.19	0.0361	21.4	0.2	0.04	14	4	8
	H	11.98	0.16	0.0256	21.7	0.5	0.25	21	5	10
	Me	11.82	0	0	21.2	0	0	8	4	24
	Br	12.18	0.36	0.1296	21.3	0.1	0.01	38	6	1
	F	11.99	0.17	0.0289	21.9	0.7	0.49	14	4	9
	OMe	11.71	-0.11	0.0121	21.6	0.4	0.16	14	3	38
	CF_3	12.55	0.73	0.5329	21.2	0	0	71	11	14

[a]The LDP value for OEt was used.

To perform the least squares fit to the equilibrium data with various models, the parameters and data were set up as matrices. For example, for a model using Eq. 2 reproduced below

$$K_{eq} = a + b\Delta LDP + c\Delta LDP^2$$

There will be a vector matrix of K_{eq} values, which we will call ***y***, one value for each ligand investigated. The matrix ***y*** in this case is as shown below.

$$\boldsymbol{y} = \begin{bmatrix} 1120 \\ 495 \\ 1830 \\ 835 \\ 14 \\ 21 \\ 8 \\ 38 \\ 14 \\ 14 \\ 71 \end{bmatrix}$$

Corresponding to these K_{eq} values, there are a series of parameters, ΔLDP and ΔLDP^2. These are also used to generate a matrix. In the first column is a set of "1" values, which will generate the parameter *a* in Eq. 2. The second column are the *ΔLDP* values, and in the third column is the set of ΔLDP^2 values. Call this matrix ***X***.

$$\boldsymbol{X} = \begin{bmatrix} 1 & -2.48 & 6.15 \\ 1 & -1.49 & 2.22 \\ 1 & 3.98 & 15.84 \\ 1 & 3.15 & 9.92 \\ 1 & 0.19 & 0.04 \\ 1 & 0.16 & 0.03 \\ 1 & 0 & 0 \\ 1 & 0.36 & 0.13 \\ 1 & 0.17 & 0.03 \\ 1 & -0.11 & 0.01 \\ 1 & 0.73 & 0.53 \end{bmatrix}$$

The equation to analytically determine the vector of global fitting parameters ***b*** is shown below,[7] which is the 1×3 vector matrix containing *a, b*, and *c*. The advantage of this procedure is that local minima cannot be obtained like in iterative procedures, but, generally speaking, similar values are obtained between iterative fits and this matrix operation. The matrix operations were done in Microsoft Excel.

$$(\boldsymbol{X}^T\boldsymbol{X})^{-1}\boldsymbol{X}^T\boldsymbol{y} = \boldsymbol{b}$$

The following combinations of variables were considered, shown as 5 trials in the table below, and the best overall fit resulted from simple electronic treatment of the K_{eq} data, trial 5. Fits that included the steric parameters were generally worse and were never significantly improved over the simple fit in Trial 5. In most cases, models involving steric parameters provided unphysical negative equilibrium constants as well. Consequently, the simple fit shown in Trial 5 was used.

Least Squares Fit Trial	Parameters
1	ΔLDP, $(\Delta LDP)^2$, $\Delta\%V_{bur}$
2	ΔLDP, $(\Delta LDP)^2$, $(\Delta\%V_{bur})^2$
3	ΔLDP, $(\Delta LDP)^2$, $(\Delta\%V_{bur})^2$, $\Delta\%V_{bur}$
4	$(\Delta LDP)^2$, $\Delta\%V_{bur}$
5	ΔLDP, $(\Delta LDP)^2$

The fit with the coefficients calculated is shown in Eq. 3. While Eq. 3, has a linear and a squared term in LDP, an algebraic rearrangement of this quadratic equation to the vertex form of the parabolic equation gives Eq. 4. The fit shown in Figure 4 in the manuscript is from an iterative procedure done in Kaleidagraph 4.1.3, which gives very similar values to the matrix fit.

Spectral Data

*^{1}H NMR of $Ti(OPh^{2,4\text{-di-t-butyl}})_4$ (**6e**) in C_6D_6*

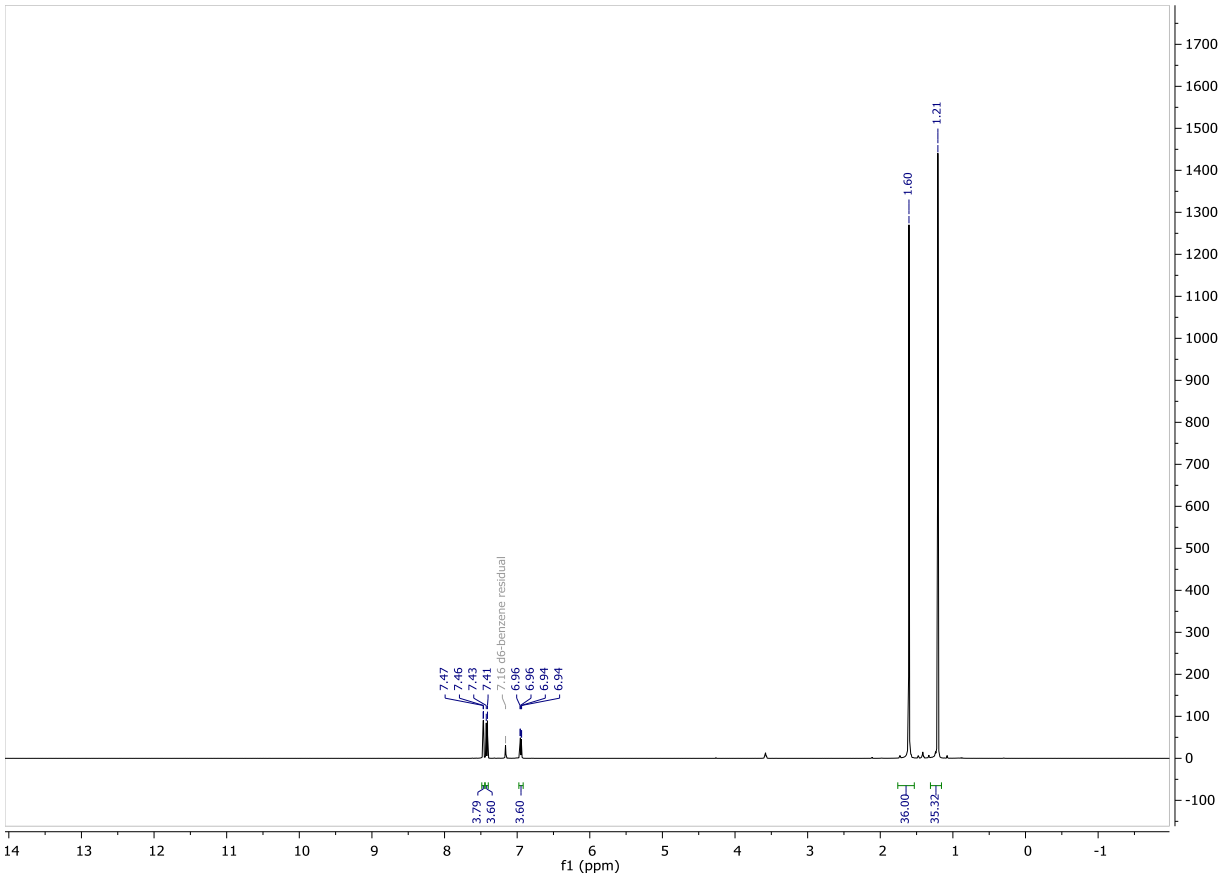

*^{13}C NMR of $Ti(OPh^{2,4\text{-di-t-butyl}})_4$ (**6e**) in C_6D_6*

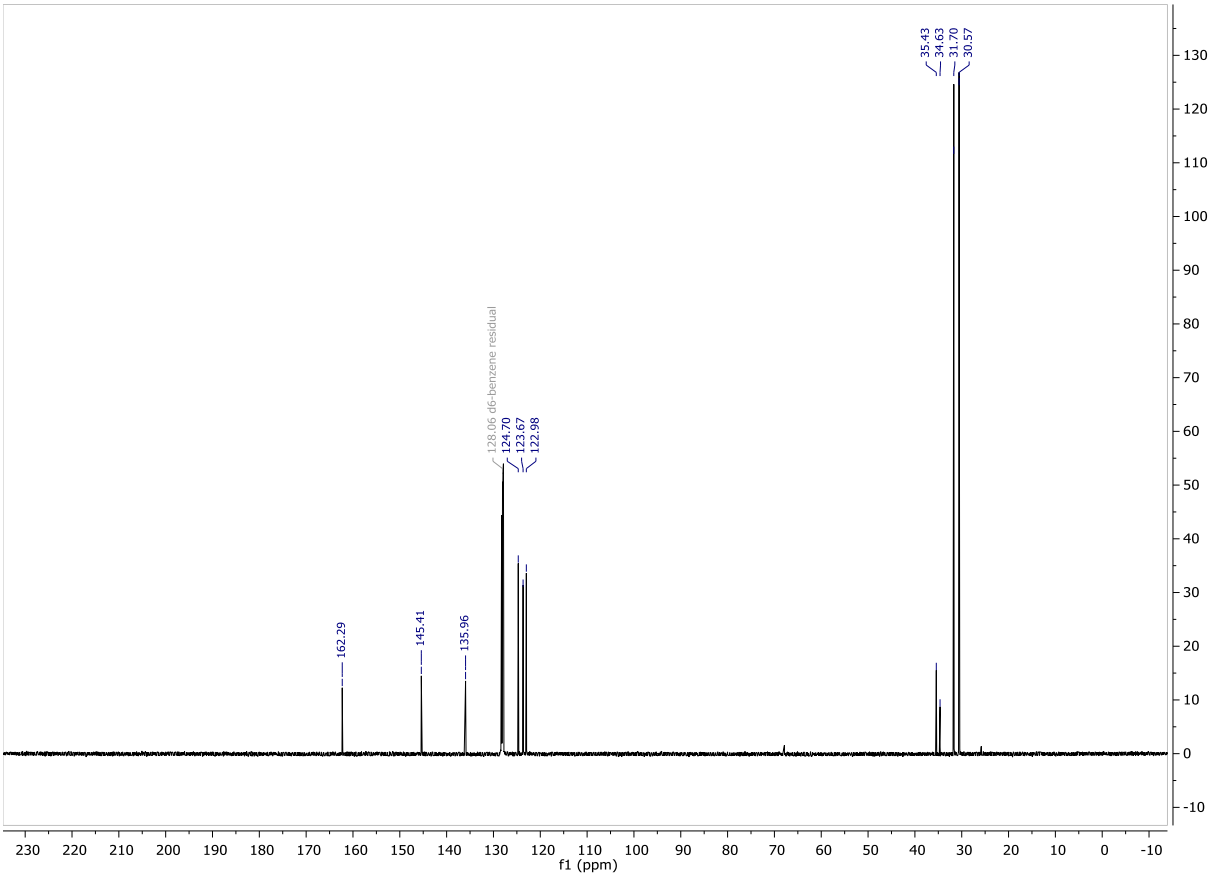

*^{1}H NMR of $Ti(OPh^{2\text{-}t\text{-}butyl})_4$ (**6c**) in C_6D_6*

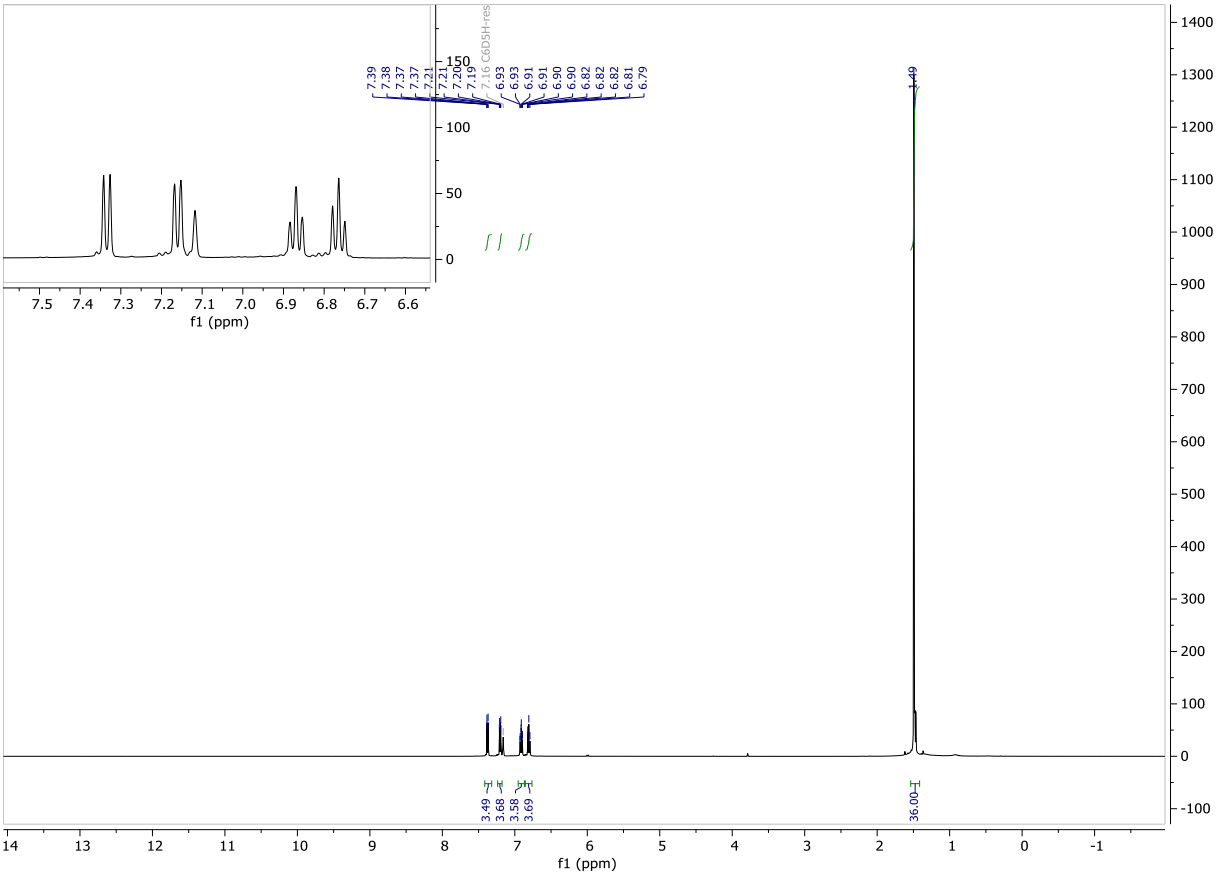

*^{13}C NMR of $Ti(OPh^{2\text{-}t\text{-}butyl})_4$ (**6c**) in C_6D_6*

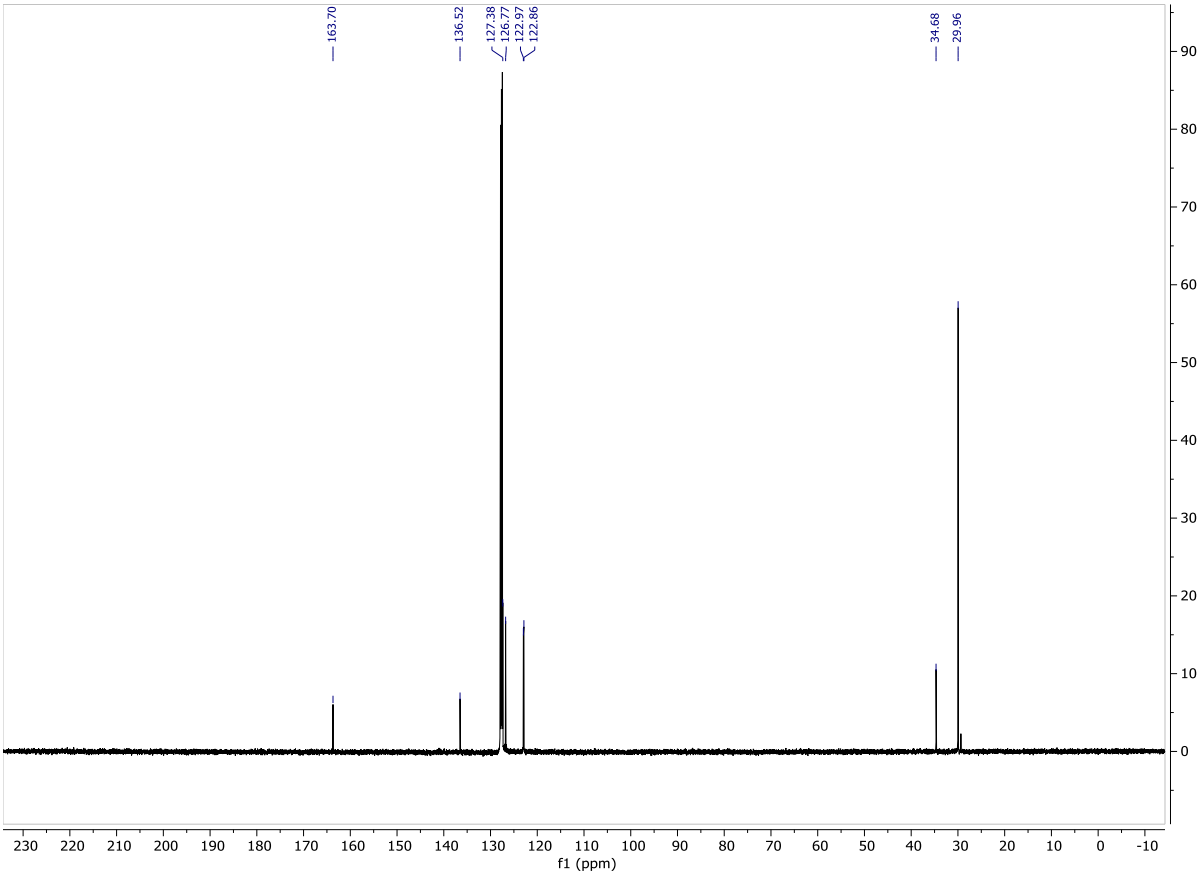

*^{1}H NMR of $Ti(OPh^{2\text{-}t\text{-}butyl\text{-}4\text{-}methoxy})_4$ (**6a**) in C_6D_6*

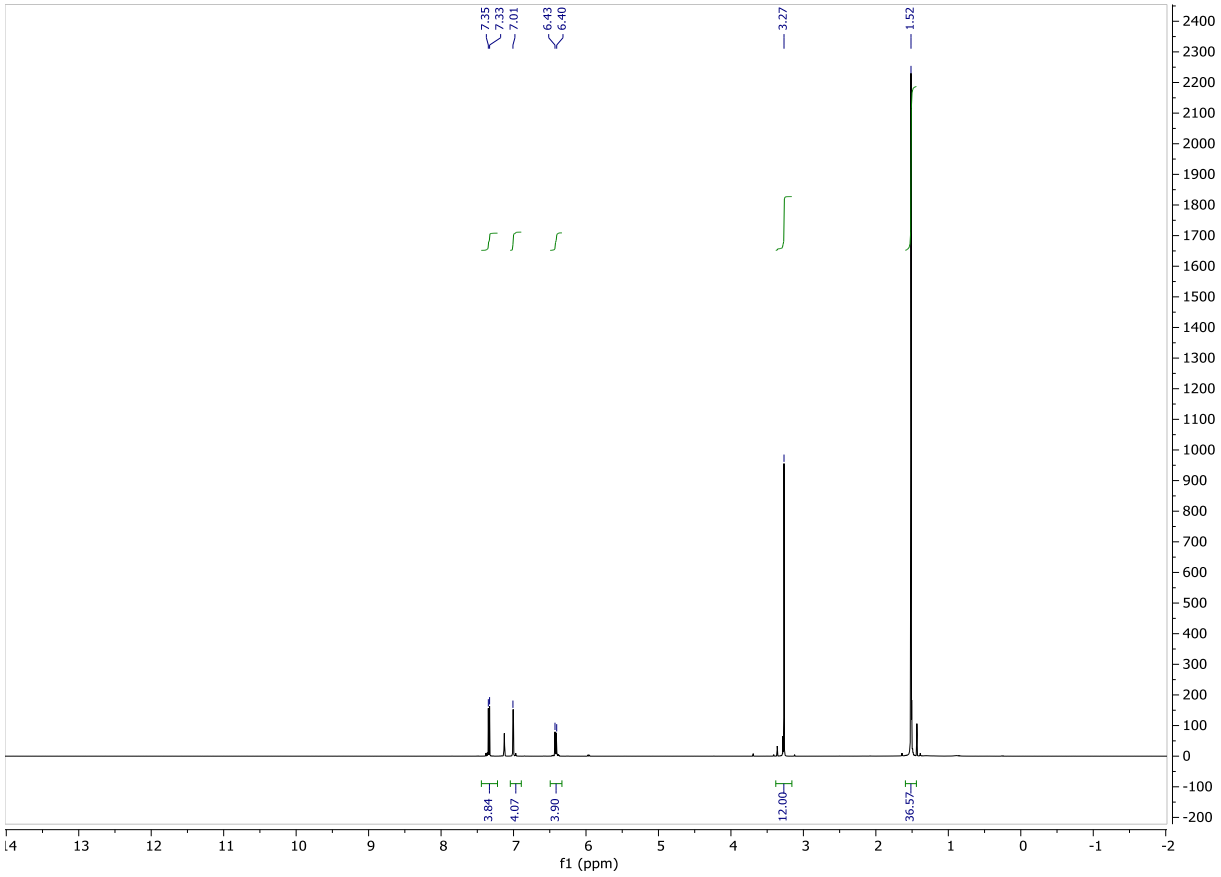

*^{13}C NMR of $Ti(OPh^{2\text{-}t\text{-}butyl\text{-}4\text{-}methoxyl})_4$ (**6a**) in C_6D_6*

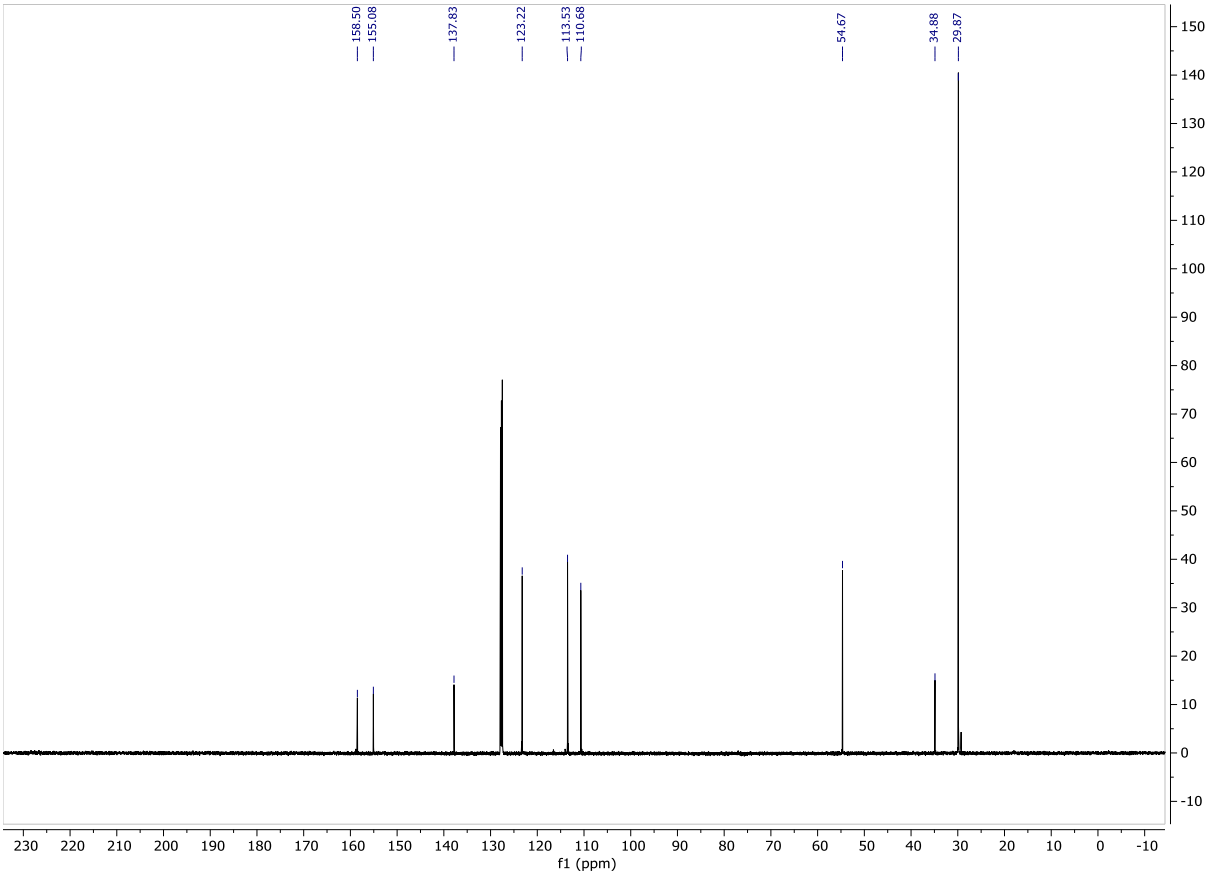

*^{1}H NMR of $Ti(OPh^{2\text{-}t\text{-}butyl\text{-}4\text{-}bromo})_4$ (**6f**) in C_6D_6*

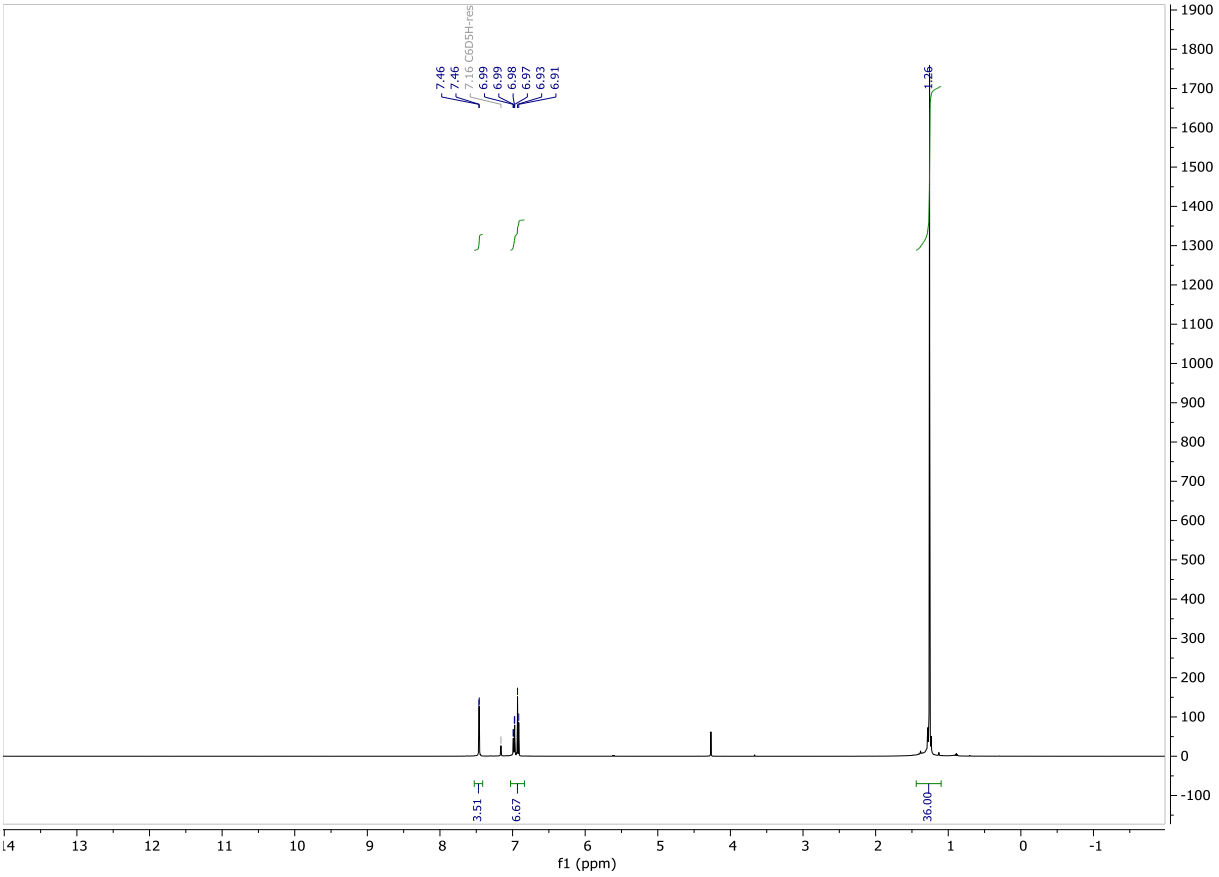

*^{13}C NMR of $Ti(OPh^{2\text{-}t\text{-}butyl\text{-}4\text{-}bromo})_4$ (**6f**) in C_6D_6*

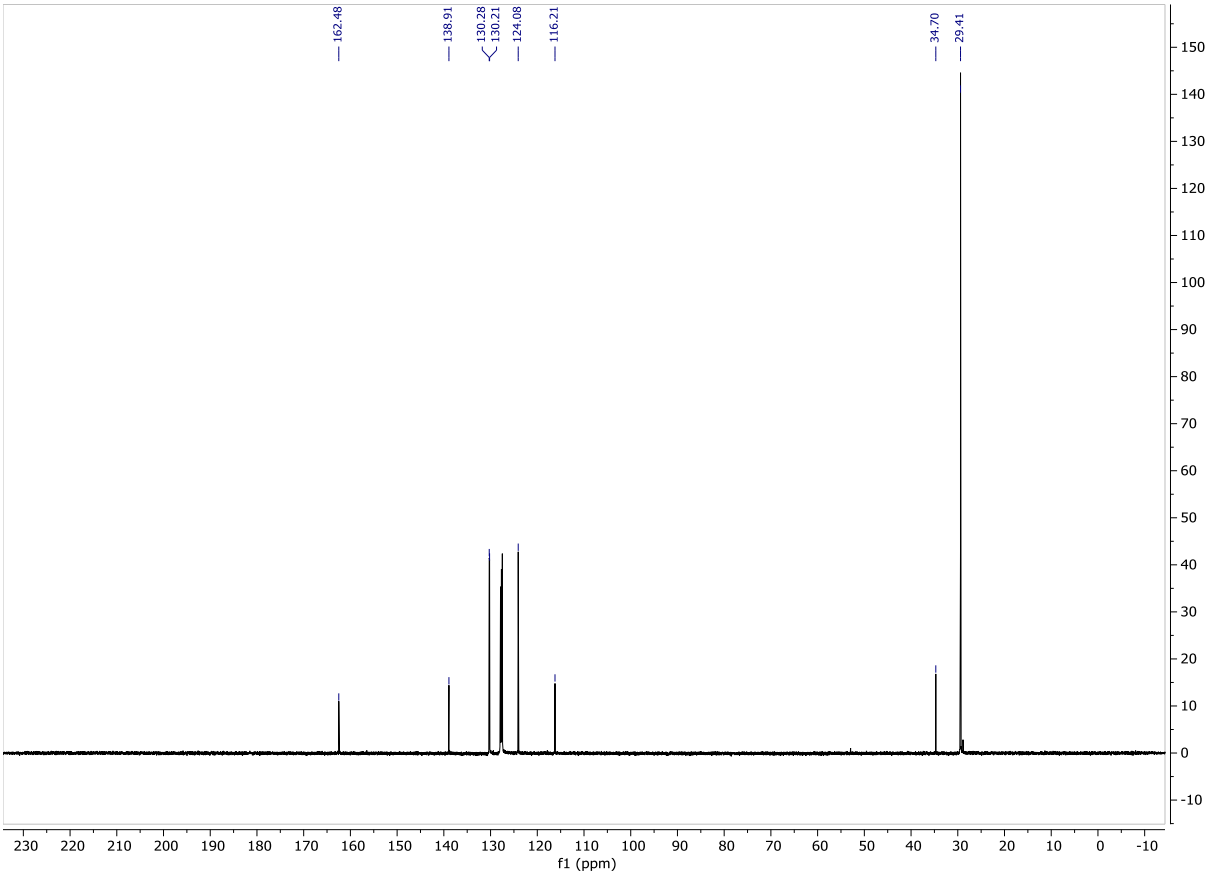

*^{1}H NMR of $Ti(OPh^{2\text{-}t\text{-}butyl\text{-}4\text{-}fluoro})_4$ (**6d**) in C_6D_6*

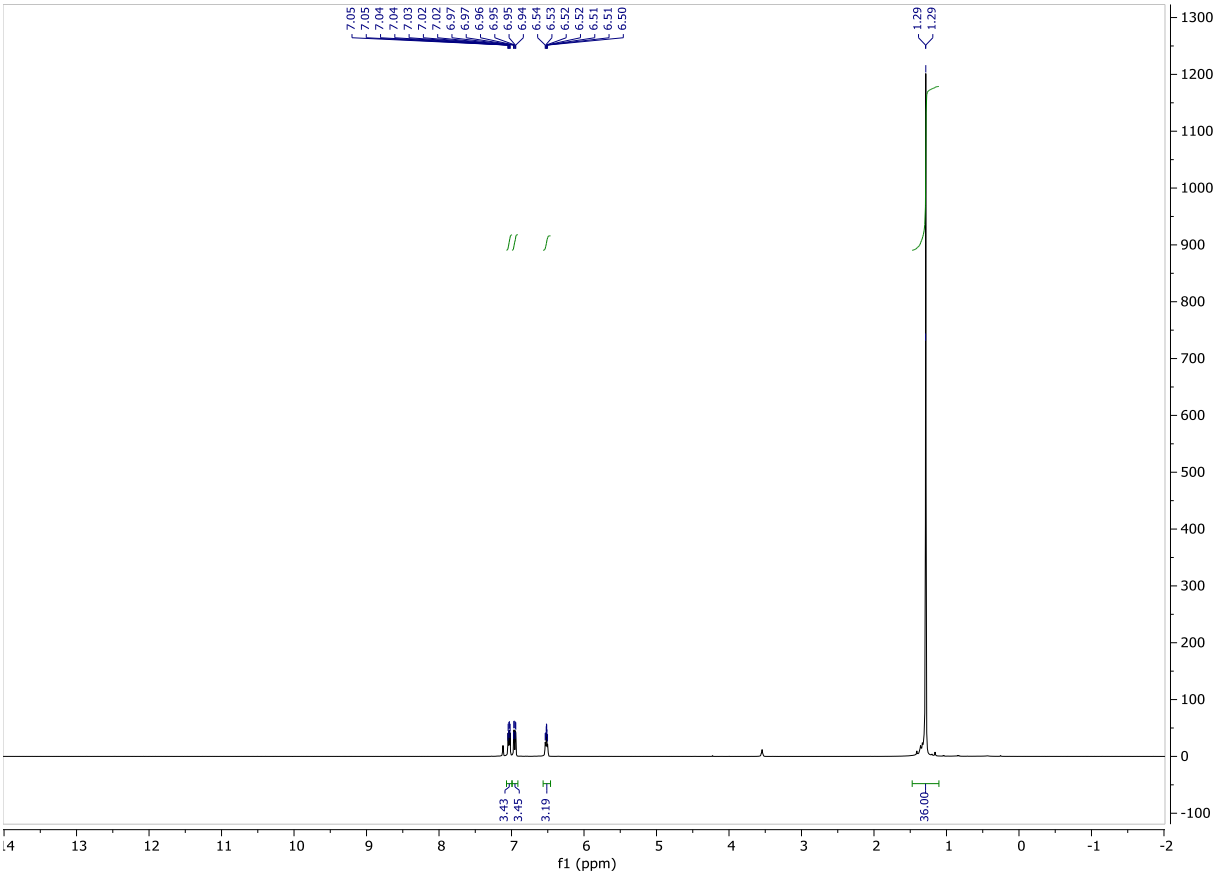

*^{13}C NMR of $Ti(OPh^{2\text{-}t\text{-}butyl\text{-}4\text{-}fluoro})_4$ (**6d**) in C_6D_6*

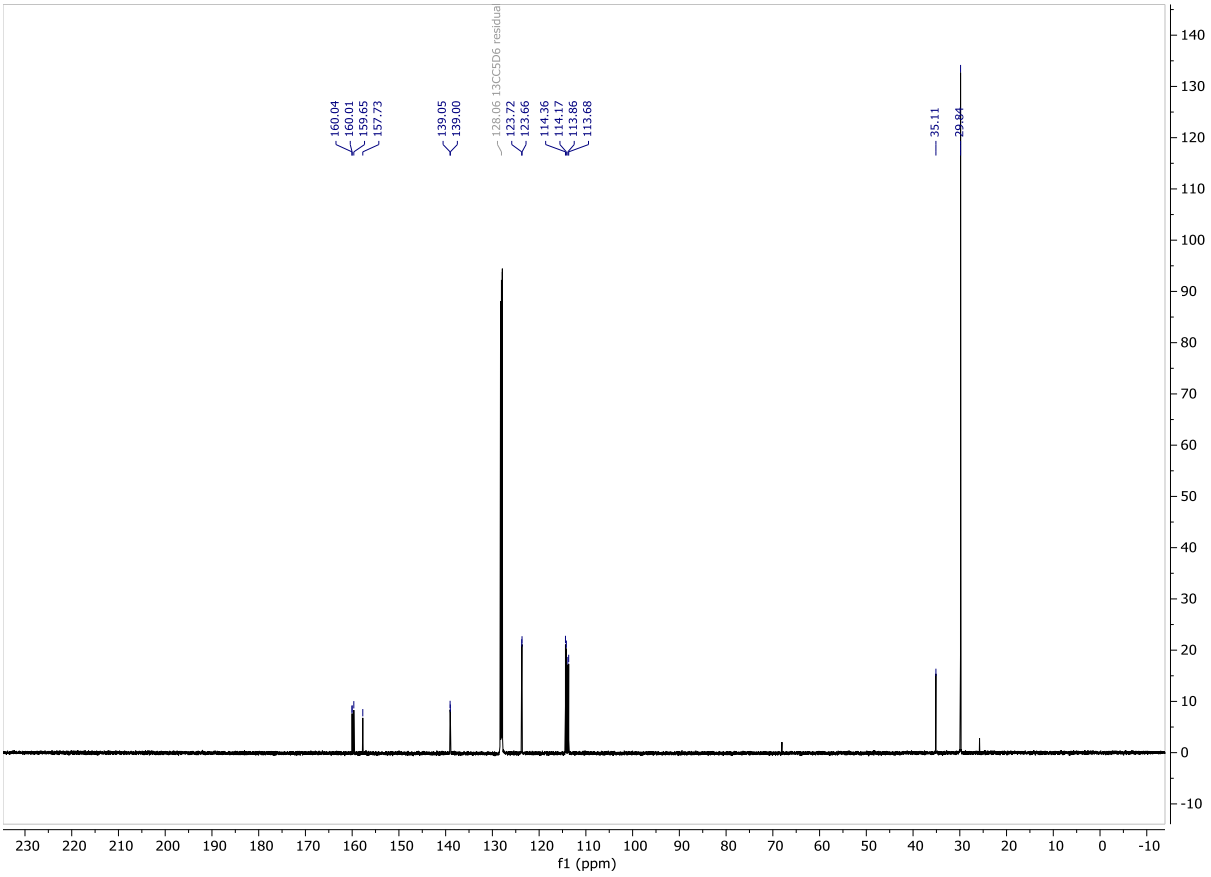

*^{19}F NMR of $Ti(OPh^{2\text{-}t\text{-}butyl\text{-}4\text{-}fluoro})_4$ (**6d**) in C_6D_6*

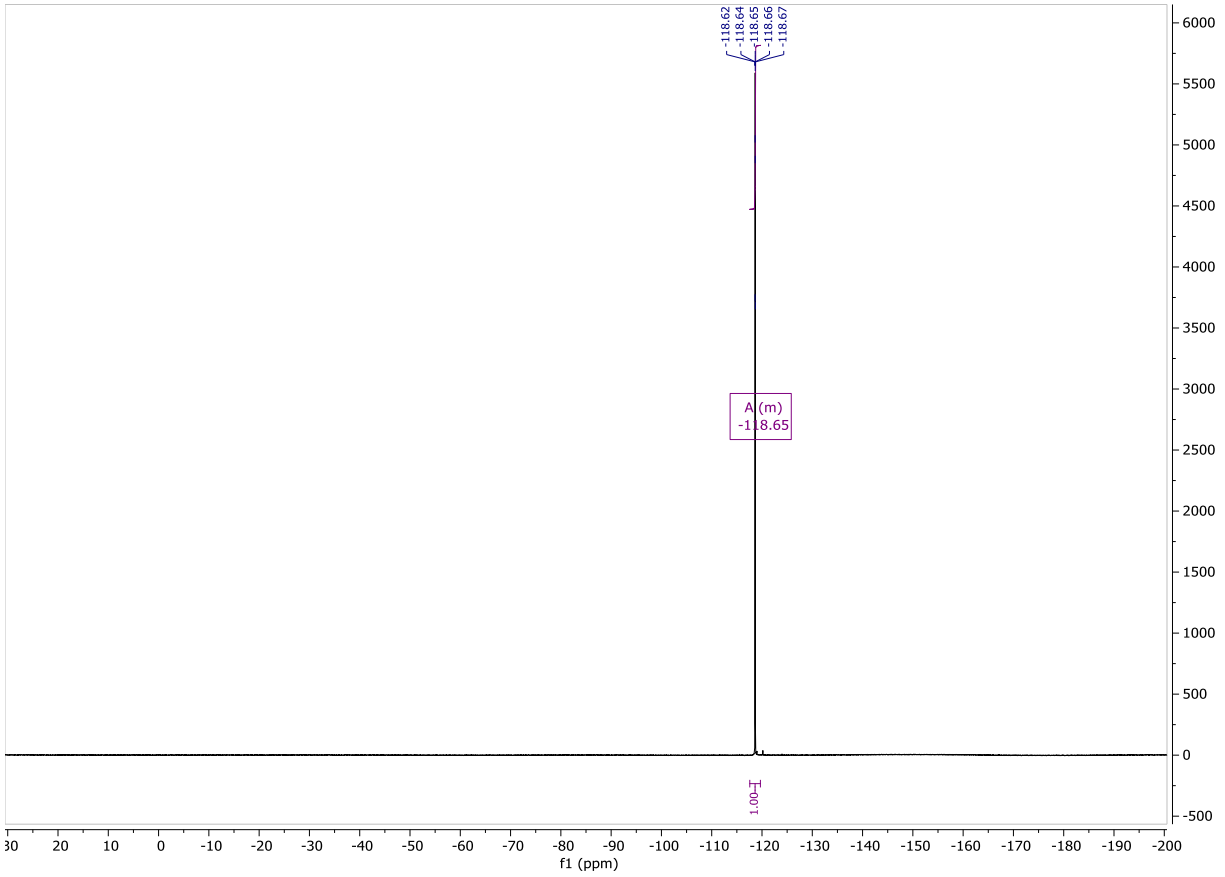

*^{1}H NMR of $Ti(OPh^{2\text{-t-butyl-4-methyl}})_4$ (**6b**) in C_6D_6*

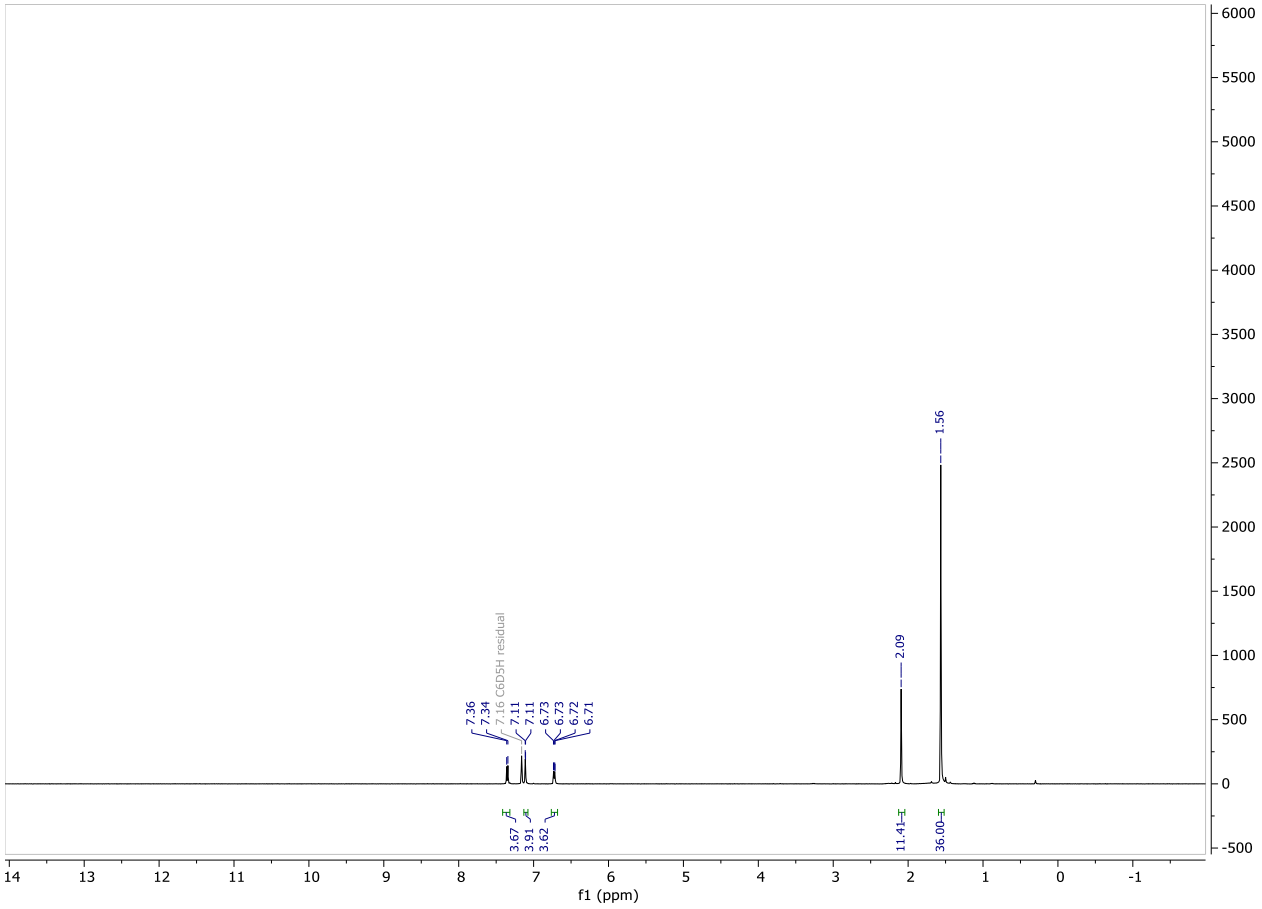

*^{13}C NMR of $Ti(OPh^{2\text{-}t\text{-}butyl\text{-}4\text{-}methyl})_4$ (**6b**) in $CDCl_3$*

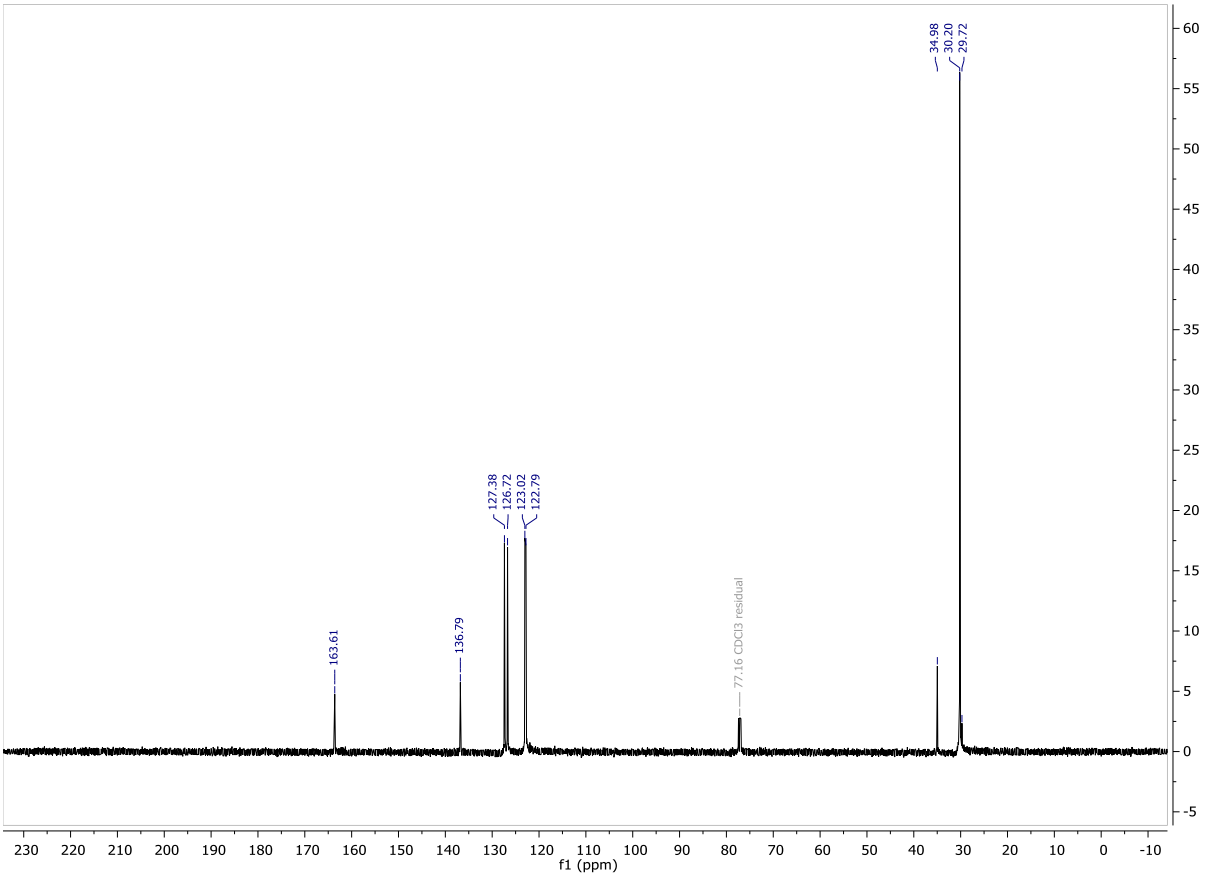

*^{1}H NMR of $Ti(OPh^{2\text{-}t\text{-}butyl\text{-}4\text{-}CF3})_4$ (**6g**) in C_6D_6*

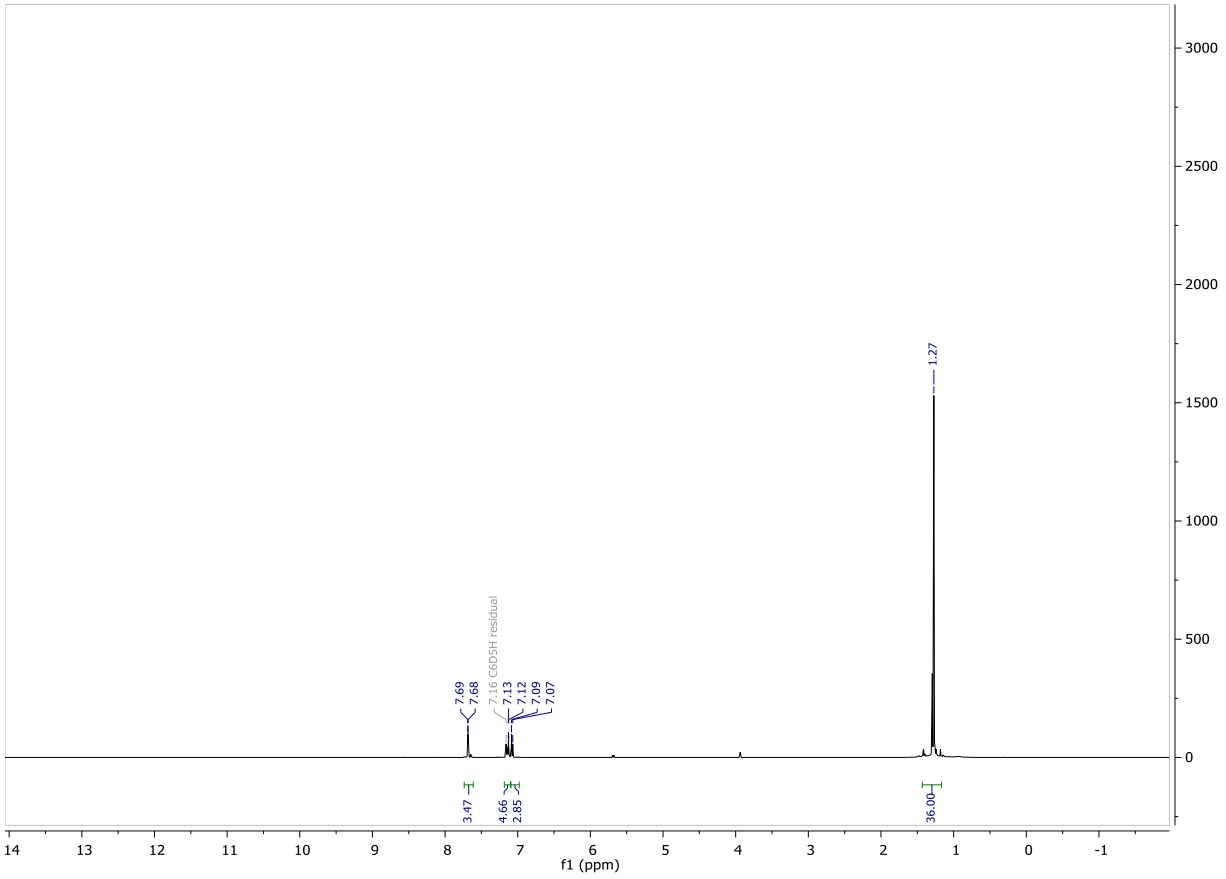

*^{13}C NMR of $Ti(OPh^{2\text{-}t\text{-}butyl\text{-}4\text{-}CF3})_4$ (**6g**) in C_6D_6*

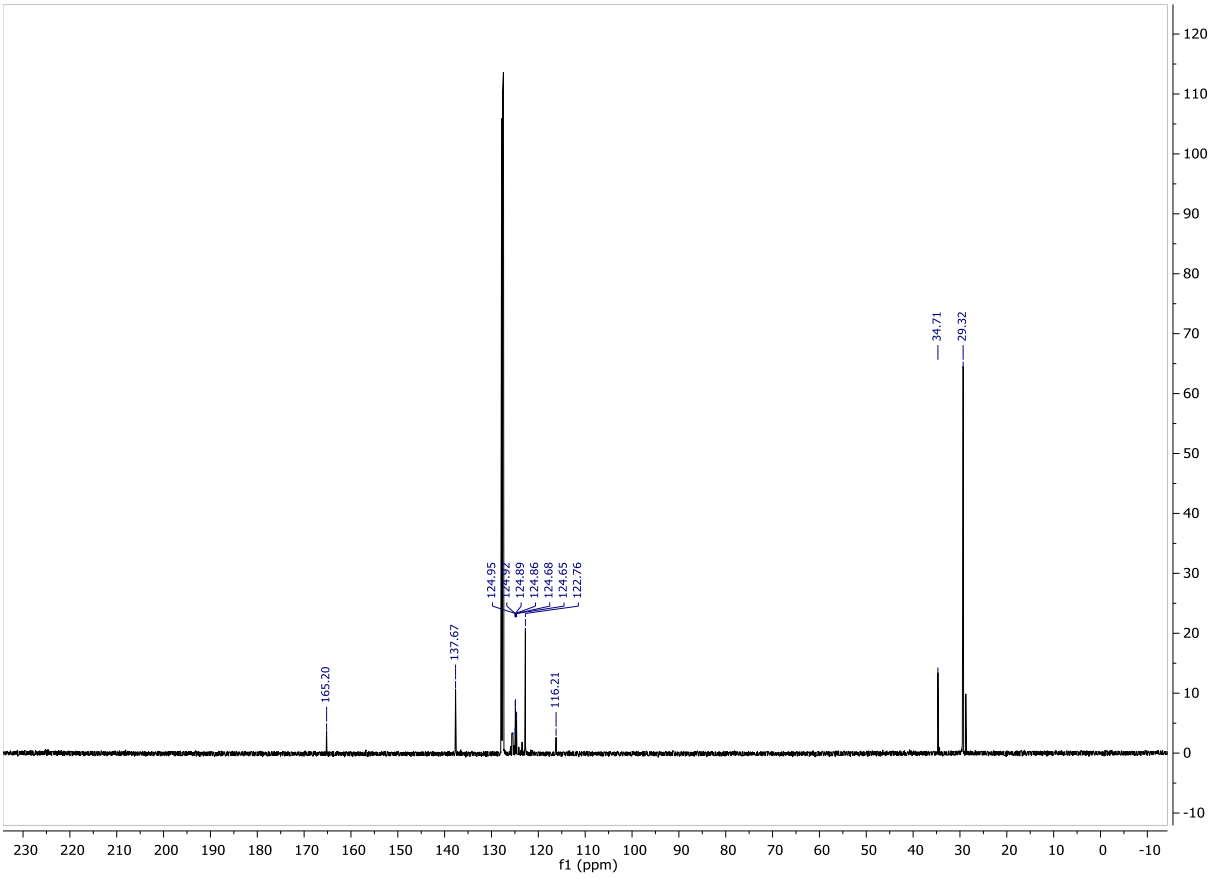

*^{19}F NMR of $Ti(OPh^{2\text{-}t\text{-}butyl\text{-}4\text{-}CF3})_4$ (**6g**) in C_6D_6*

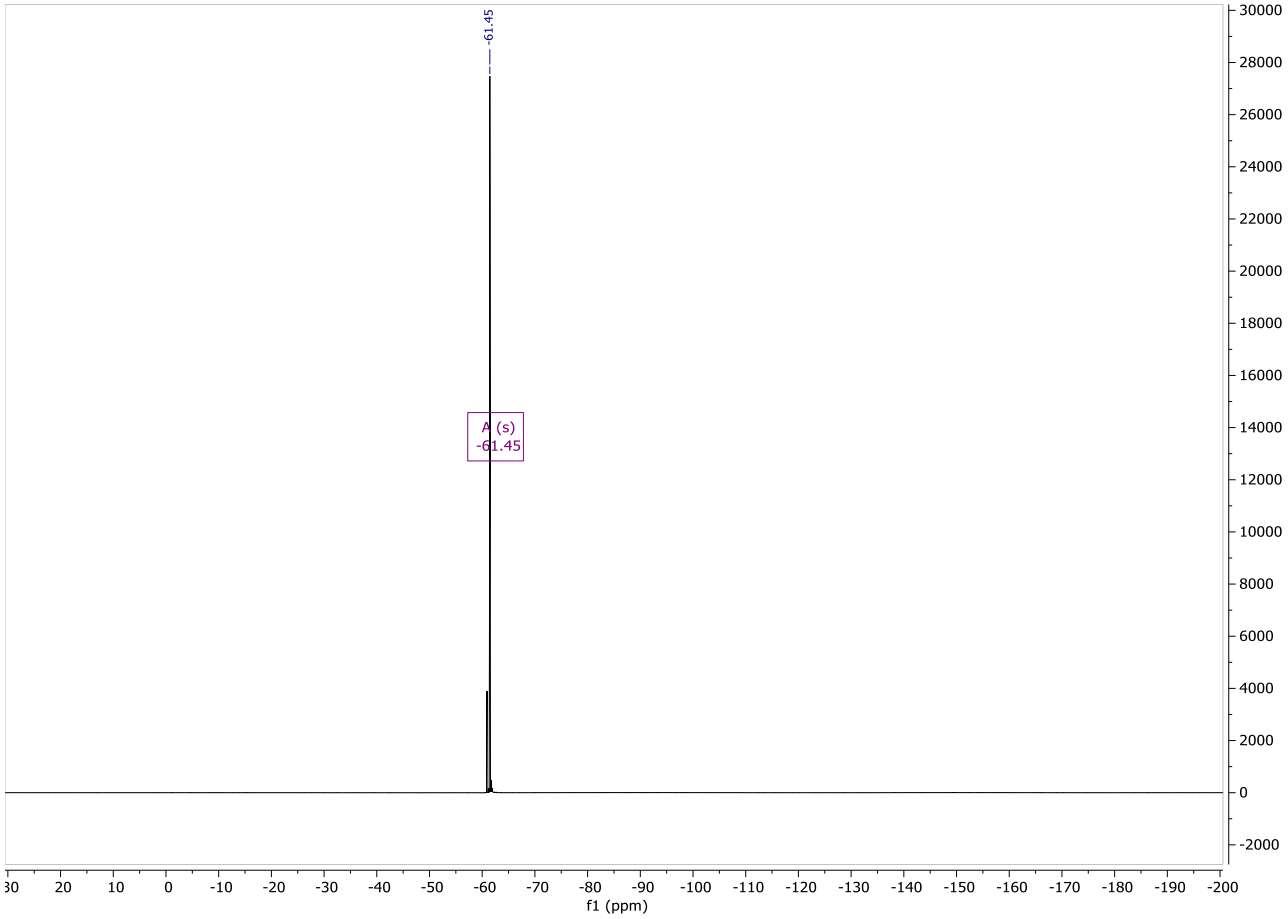

^{1}H NMR of $Ti(OArCH_2ArO)(O^{i}Pr)_2$ in $CDCl_3$

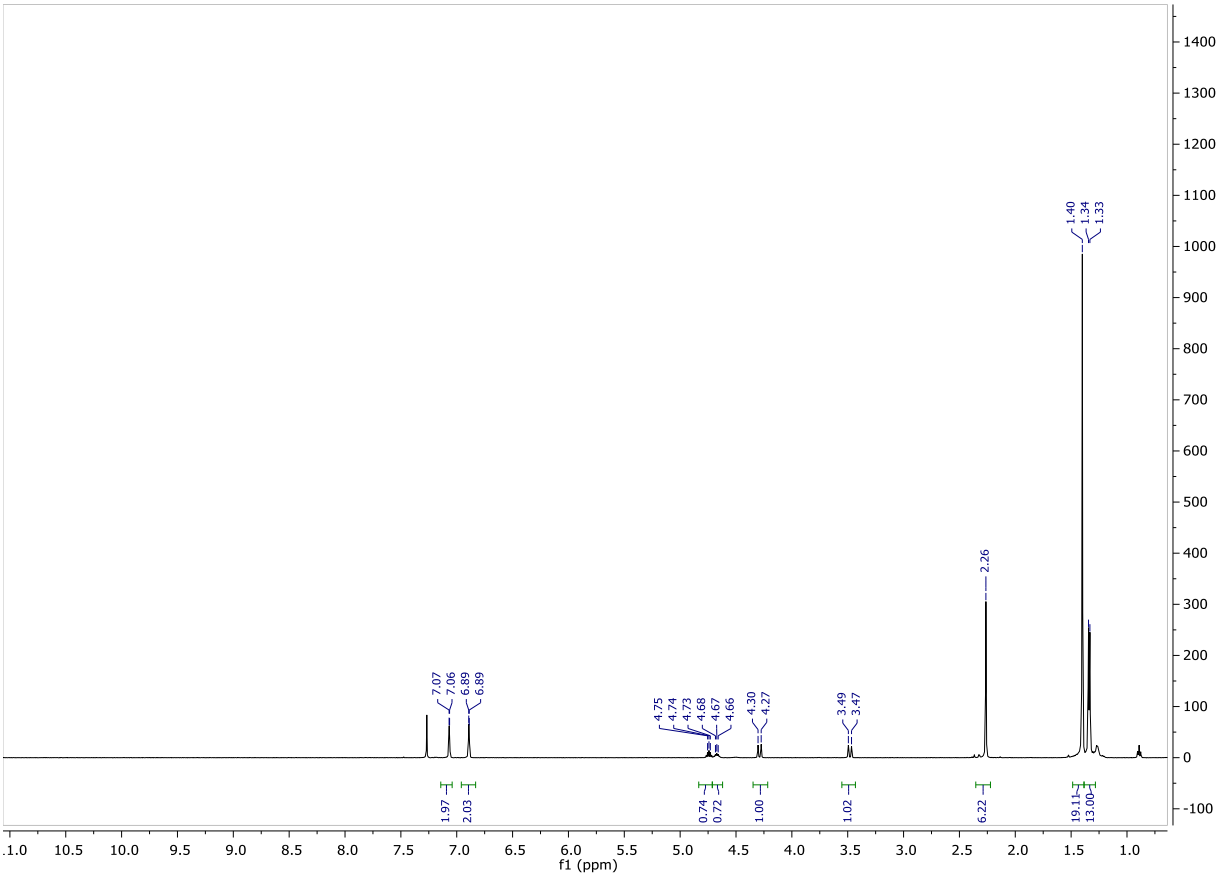

^{1}H NMR of $Ti(OArCH_2ArO)_2$ in C_6D_6

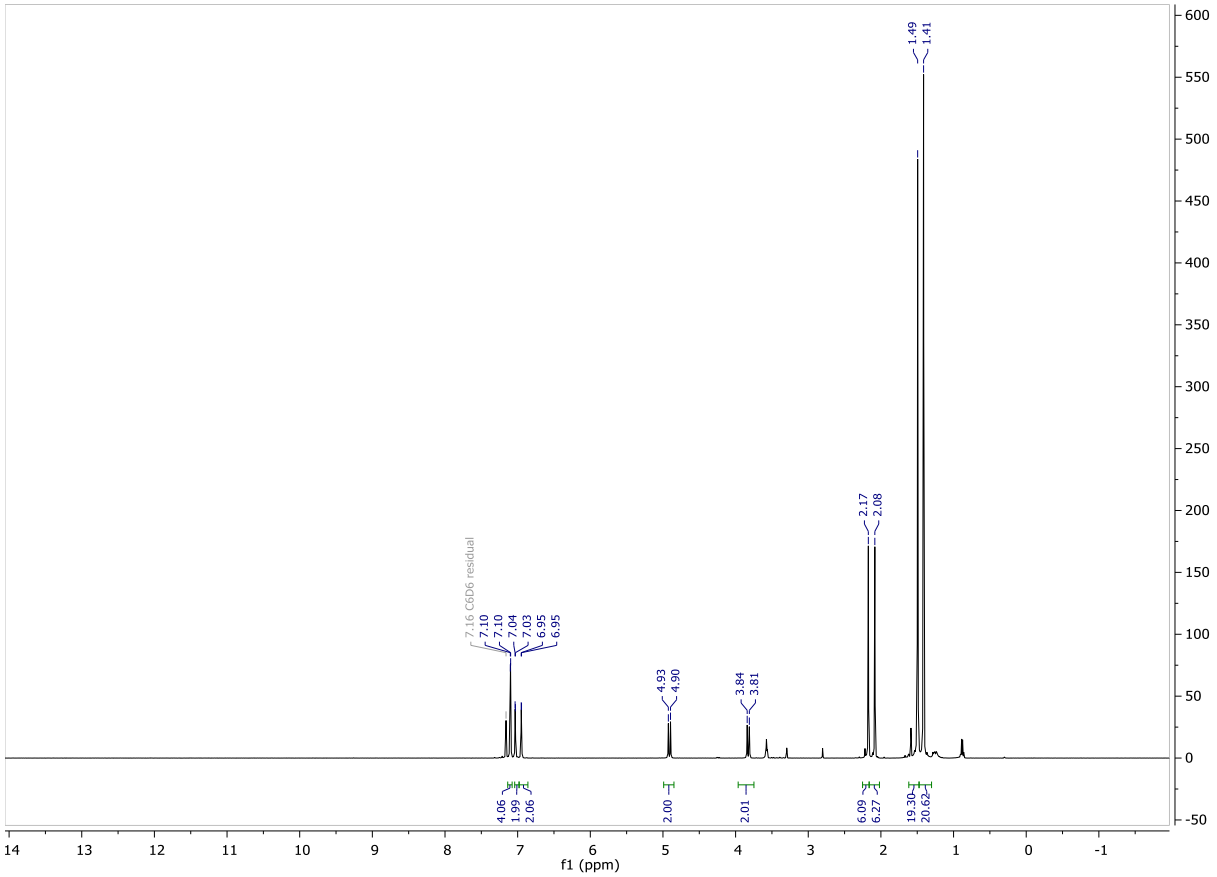

^{1}H NMR of $TiCl_2(OArCH_2ArO)$ in C_6D_6

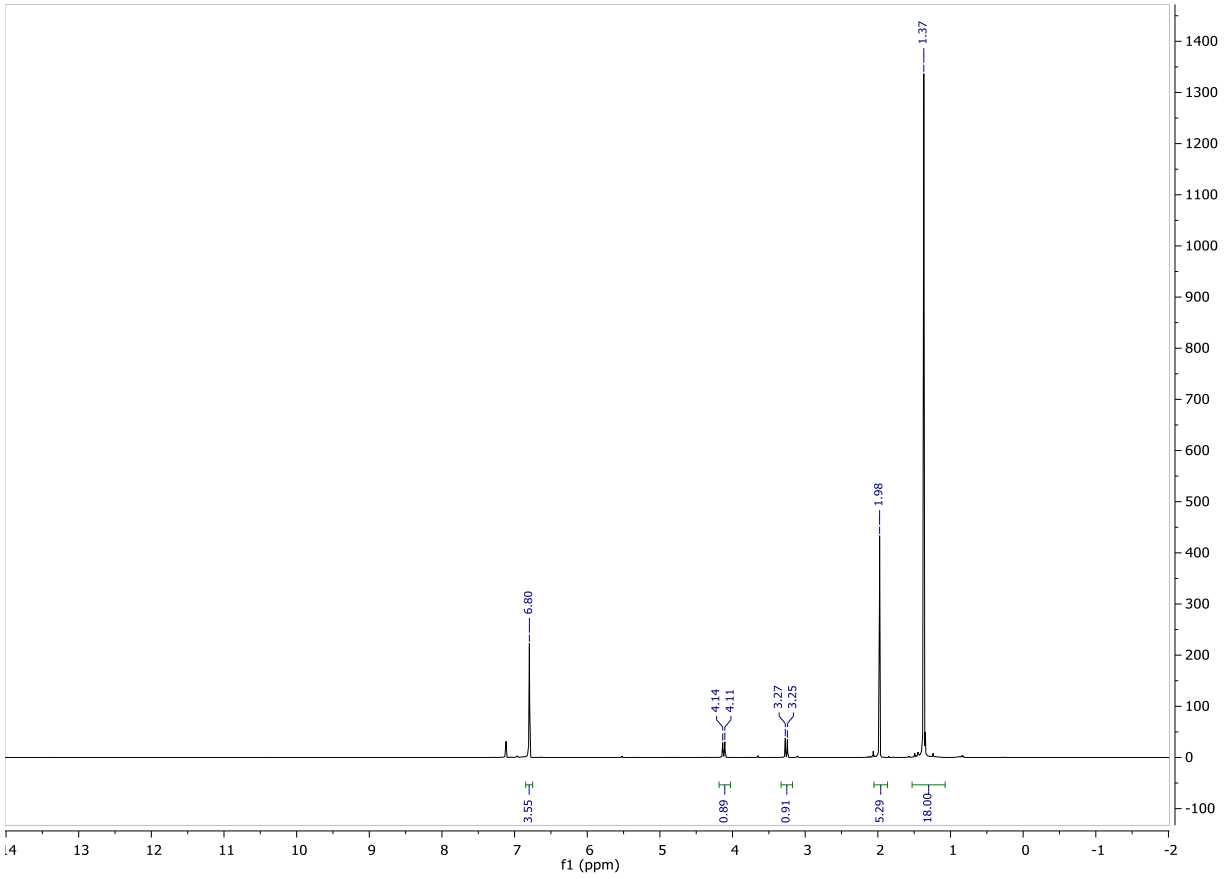

^{13}C NMR of $TiCl_2(OArCH_2ArO)$ in C_6D_6

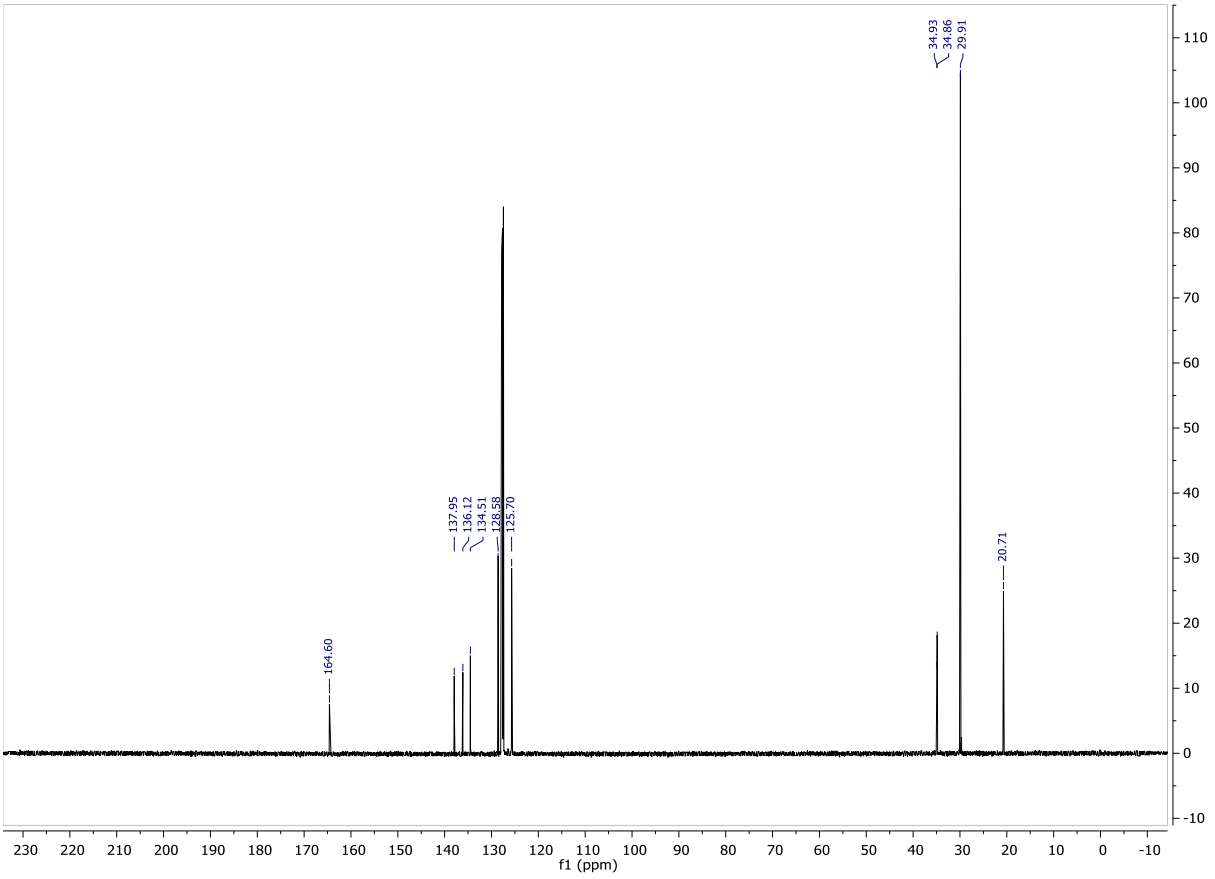

^{1}H NMR of $TiI_2(OArCH_2ArO)$ in $CDCl_3$

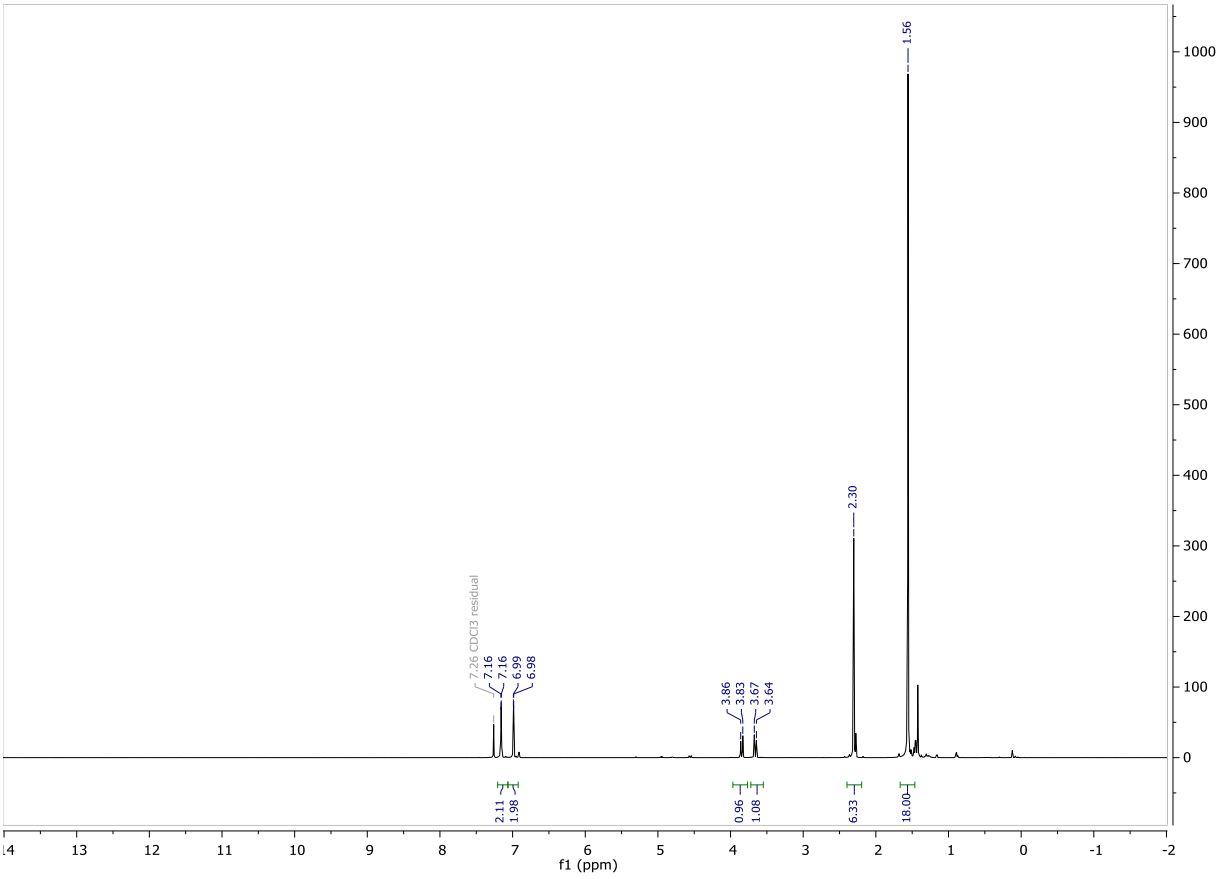

^{13}C NMR of $TiI_2(OArCH_2ArO)$ in $CDCl_3$

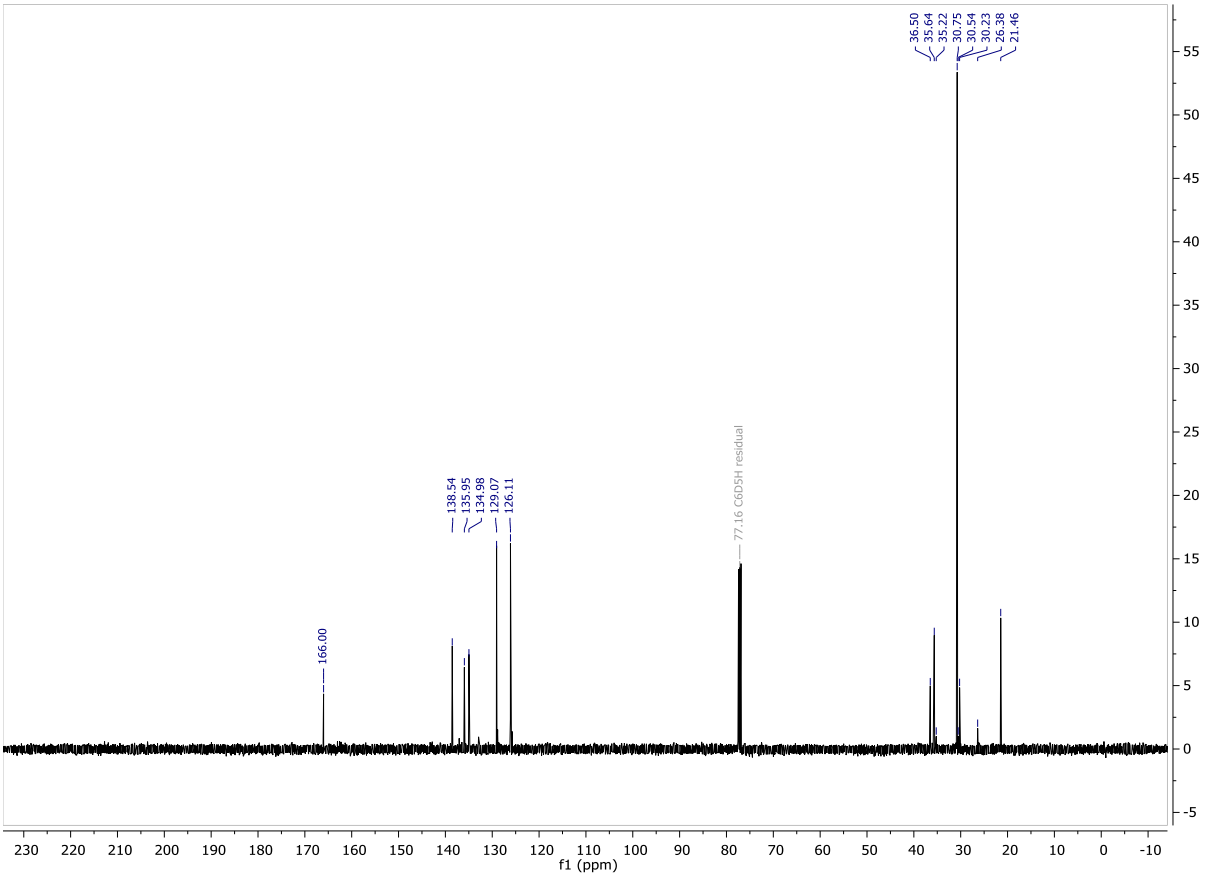

*^{1}H NMR of {Ti(OArCH$_2$ArO)(Ntolyl)}$_2$·HNMe$_2$ (**4**) in C_6D_6*

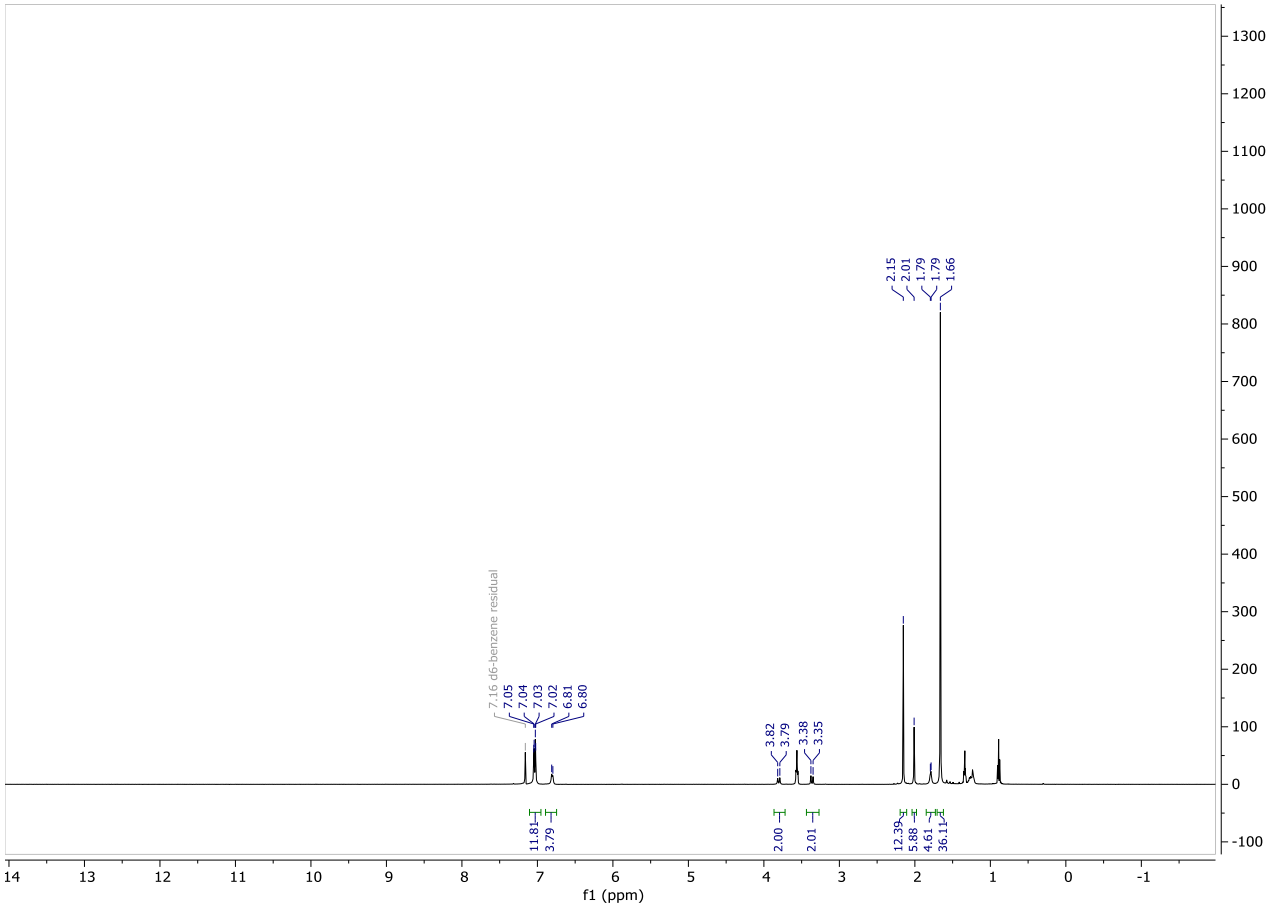

*^{13}C NMR of {Ti(OArCH$_2$ArO)(Ntolyl)}$_2$·HNMe$_2$ (**4**) in C$_6$D$_6$*

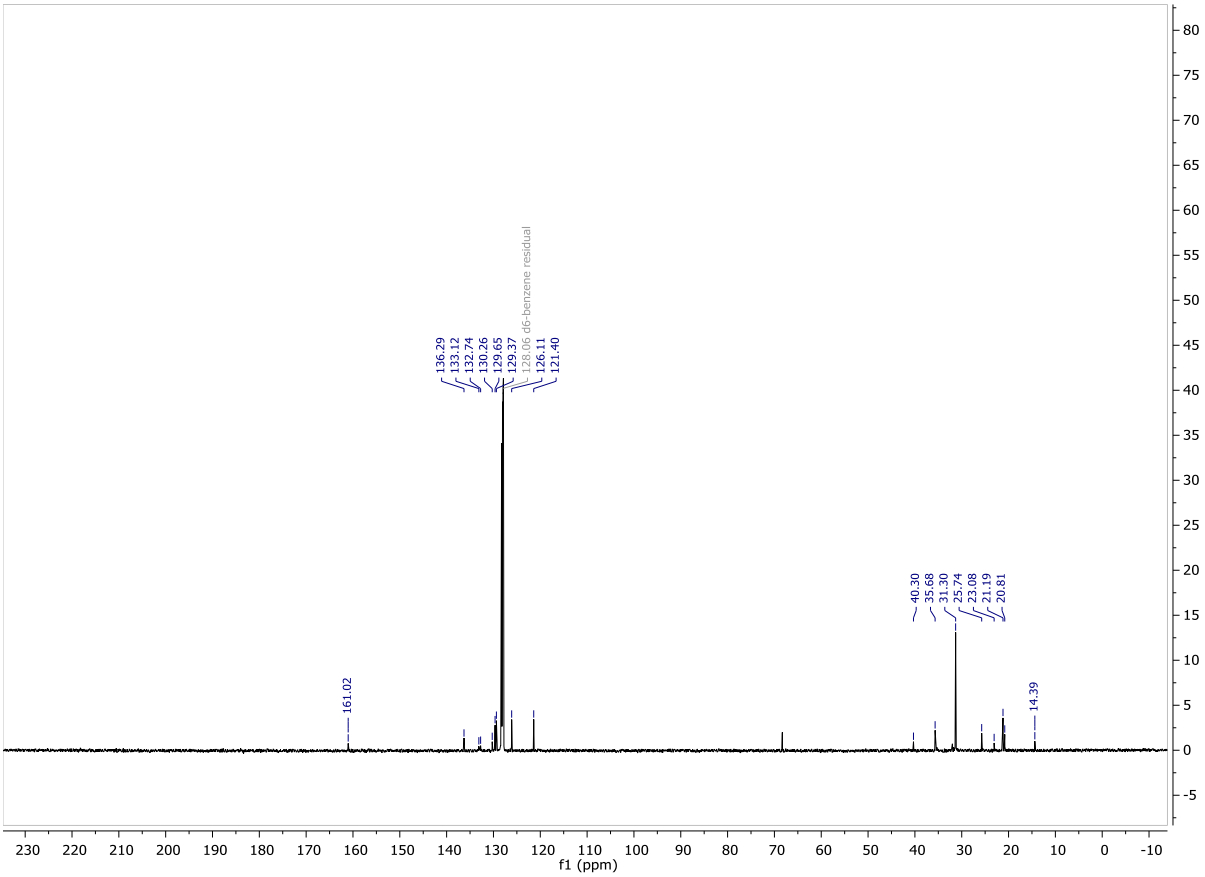

*^{1}H NMR of {Ti(μ-Ntolyl)(dpm)}$_2$ (**2**^{tol}) in toluene-d_8 room temperature*

high vac grease and hexane impurities

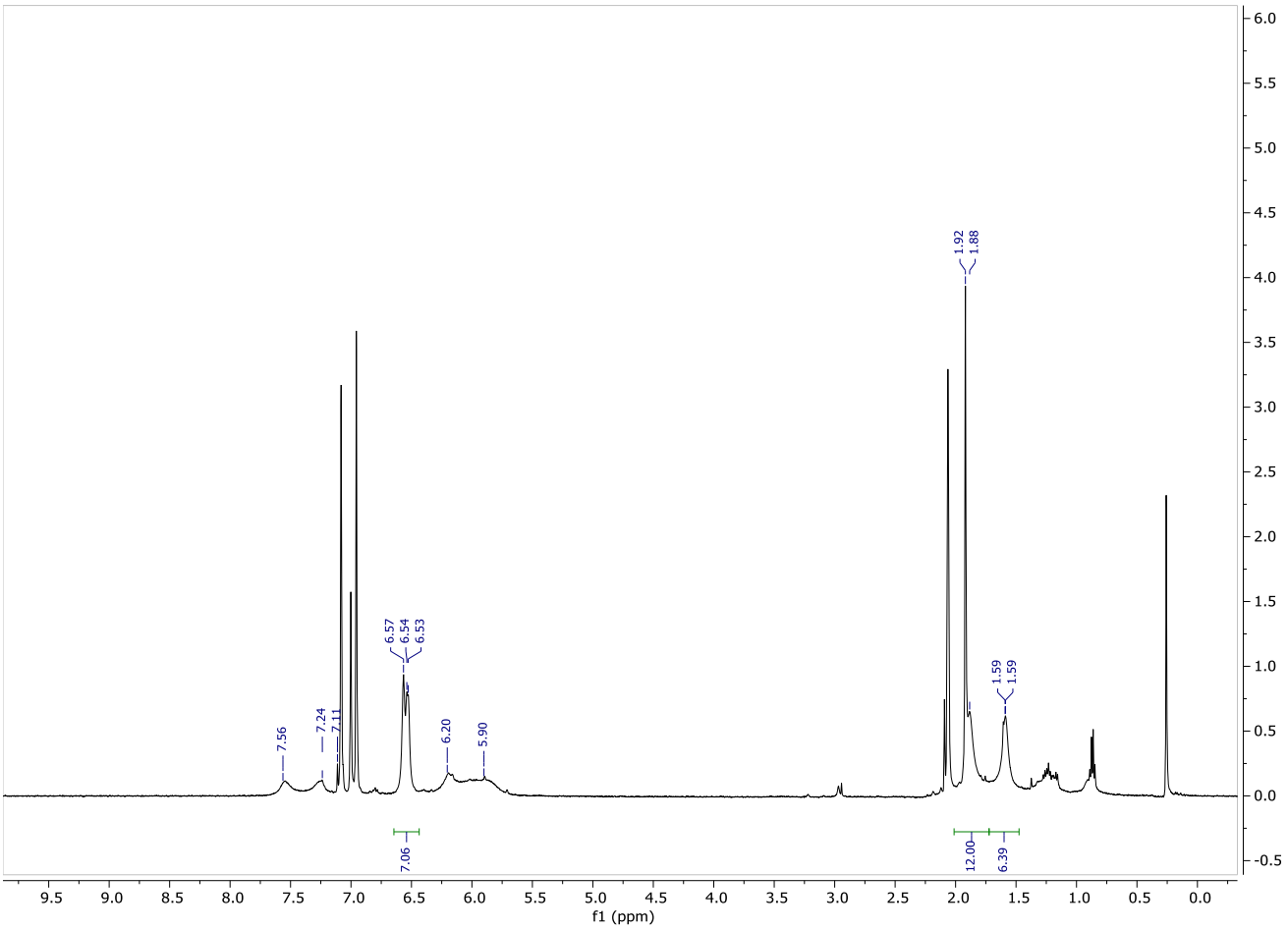

*^{1}H NMR of {Ti(μ-Ntolyl)(dpm)}$_2$ (**2^{tol}**) in toluene-d_8 at –75 °C*

high vac grease and hexane impurities

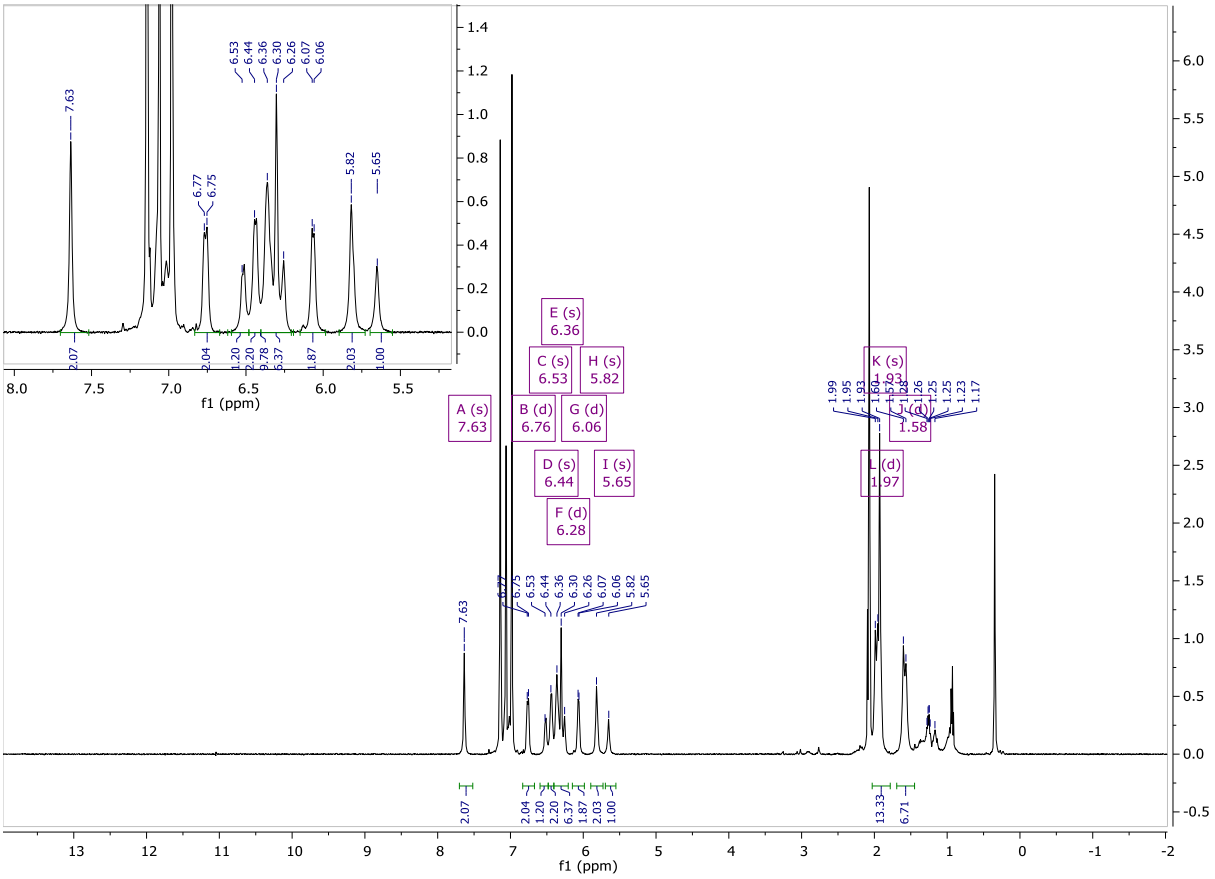

^{13}C NMR of {Ti(μ-Ntolyl)(dpm)}$_2$ in toluene-d_8 at room temperature

high vac grease and hexane impurities

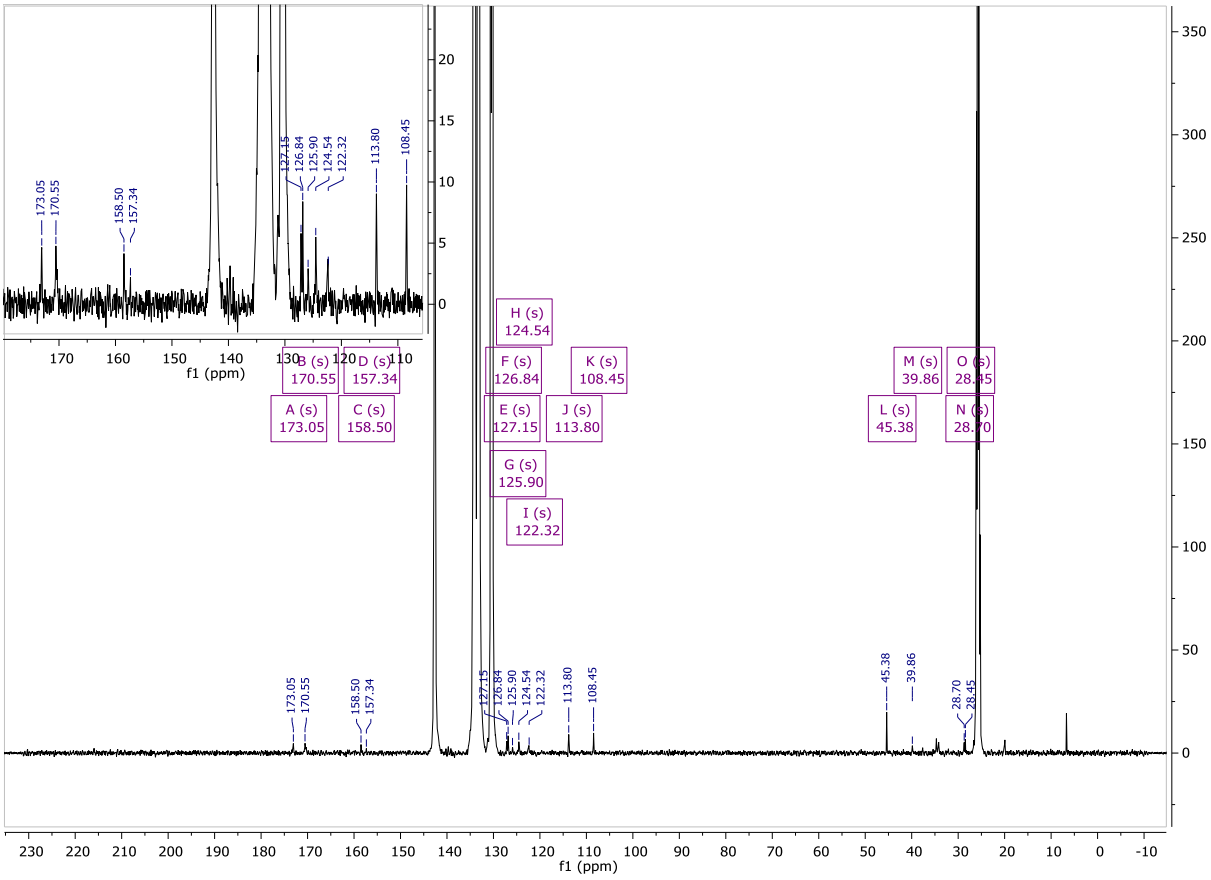

^{1}H NMR of isomeric mixture of 3CC product from the coupling of aniline, ^{t}BuNC, and 1-octyne in $CDCl_3$

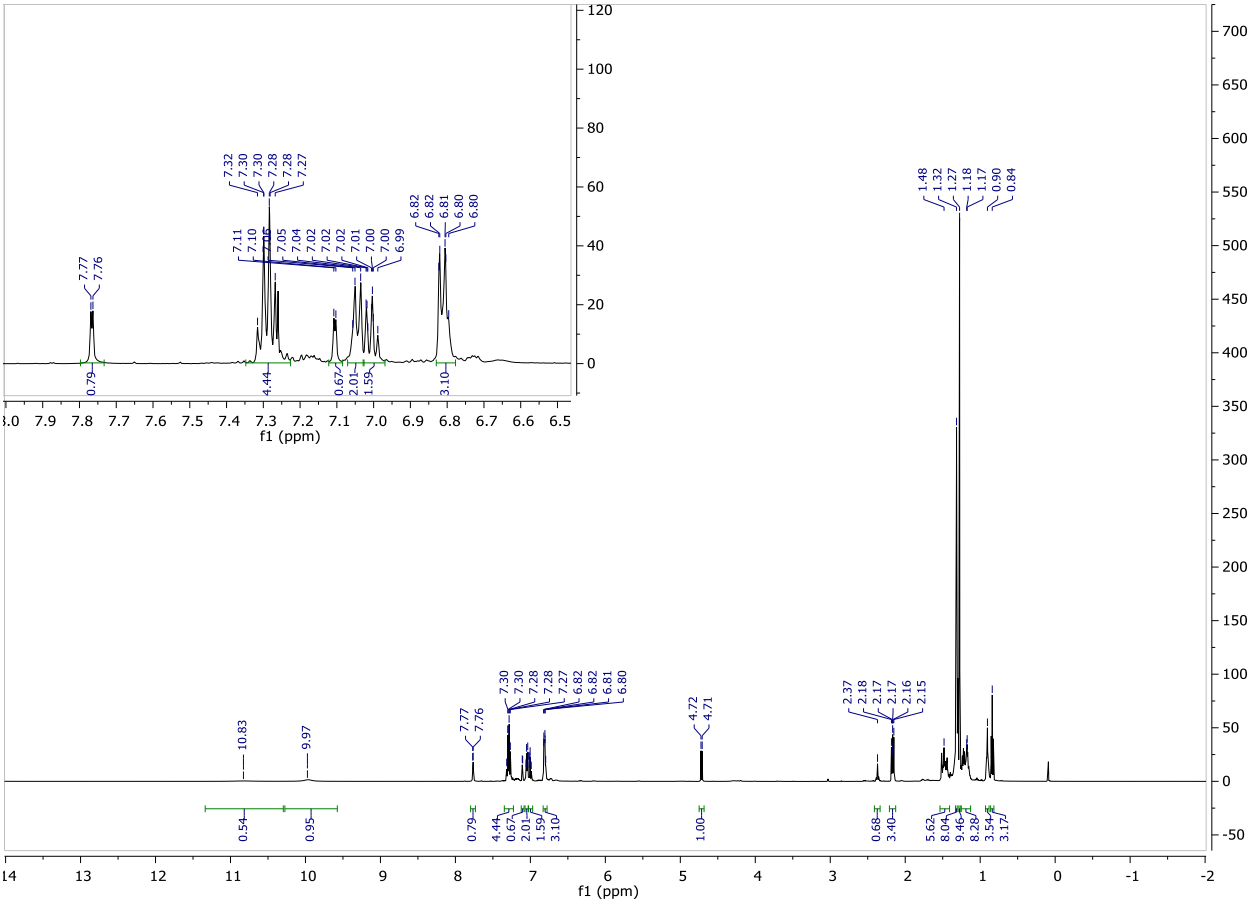

^{13}C NMR of isomeric mixture of iminoamination product from the coupling of aniline, ^{t}BuNC, and 1-octyne in $CDCl_3$

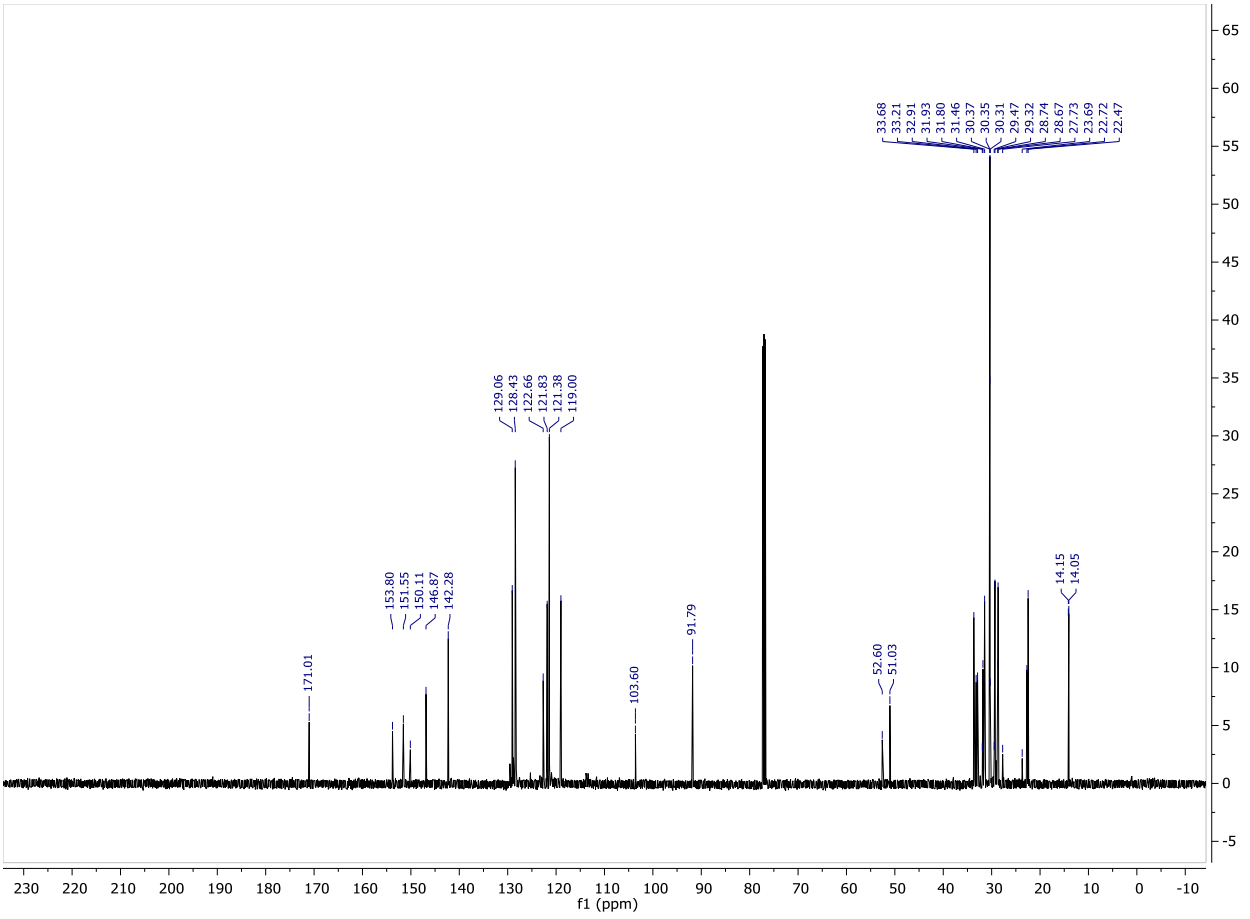

GCMS of iminoamination product isomers A and B; fragmentation pattern for A isomer

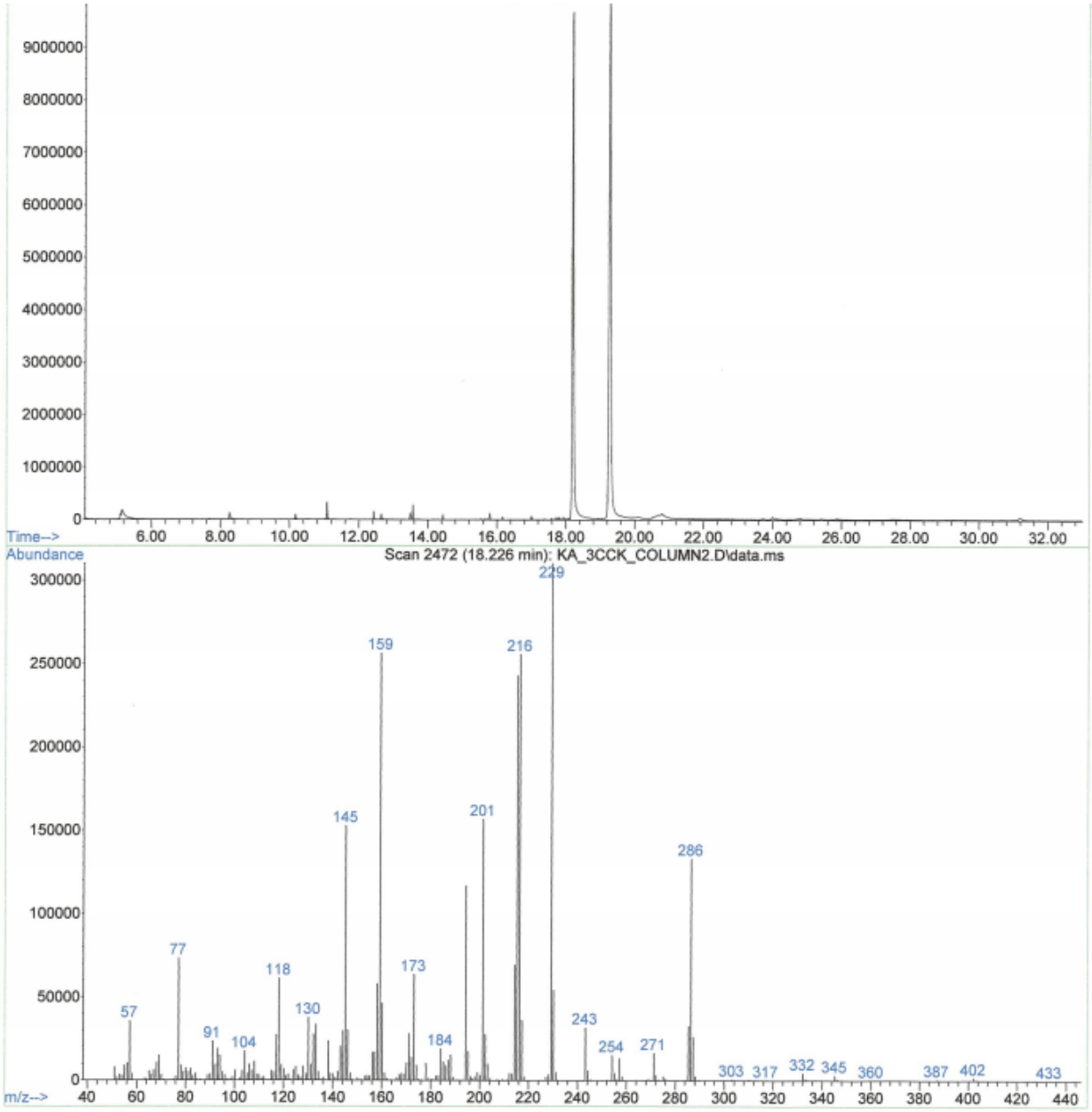

GCMS of iminoamination product isomers A and B; fragmentation pattern for B isomer

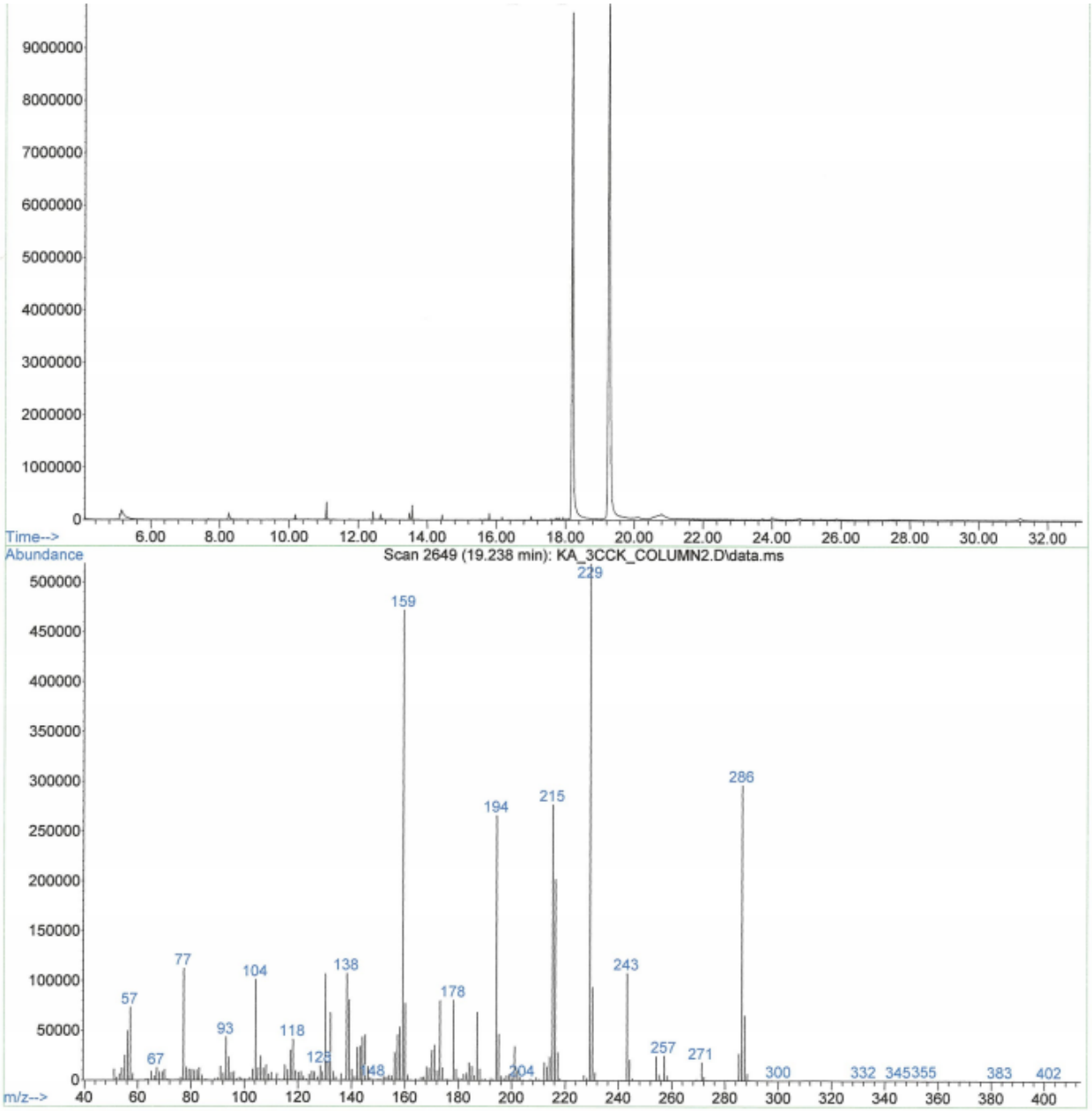

^{1}H NMR of the 4CC product in $CDCl_3$

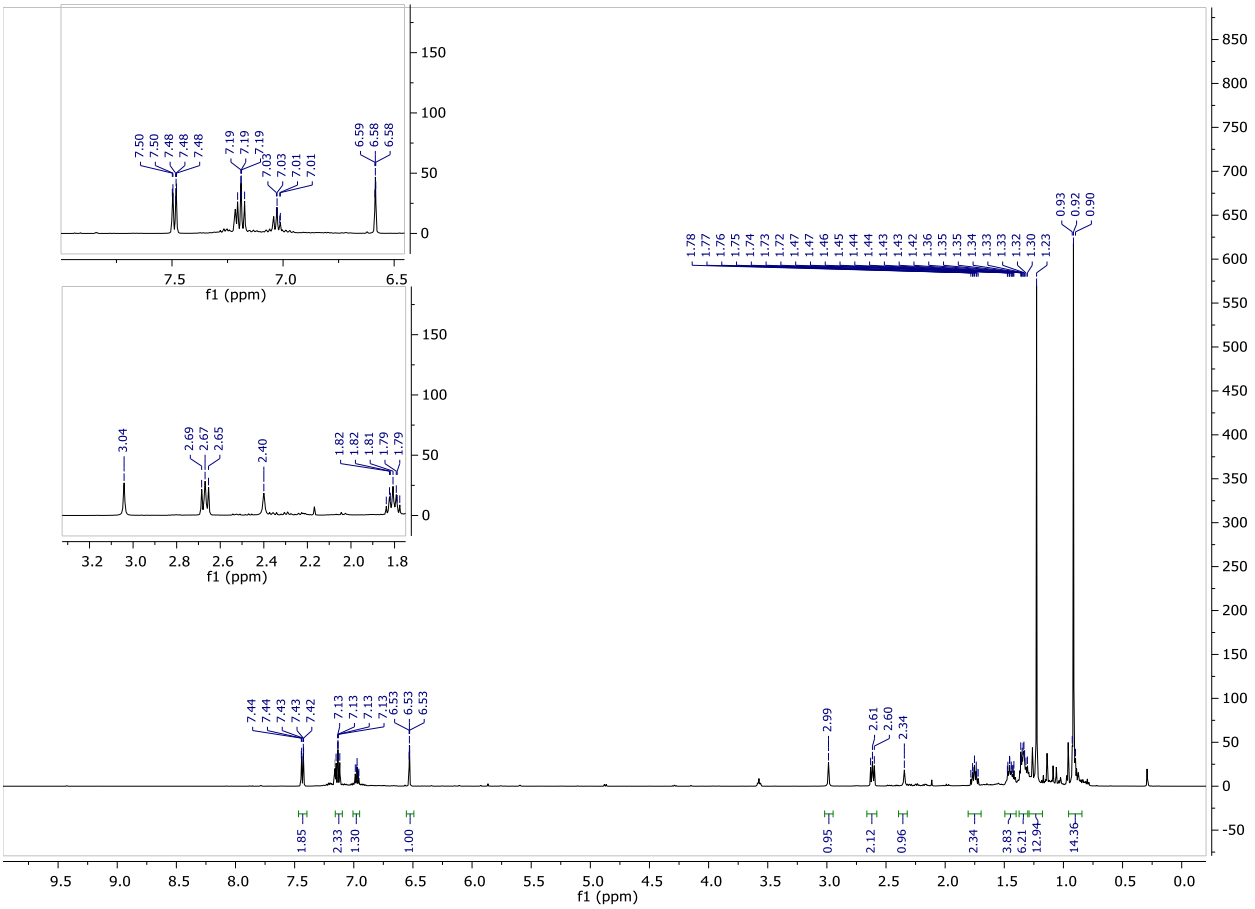

^{13}C NMR of the 4CC product in $CDCl_3$

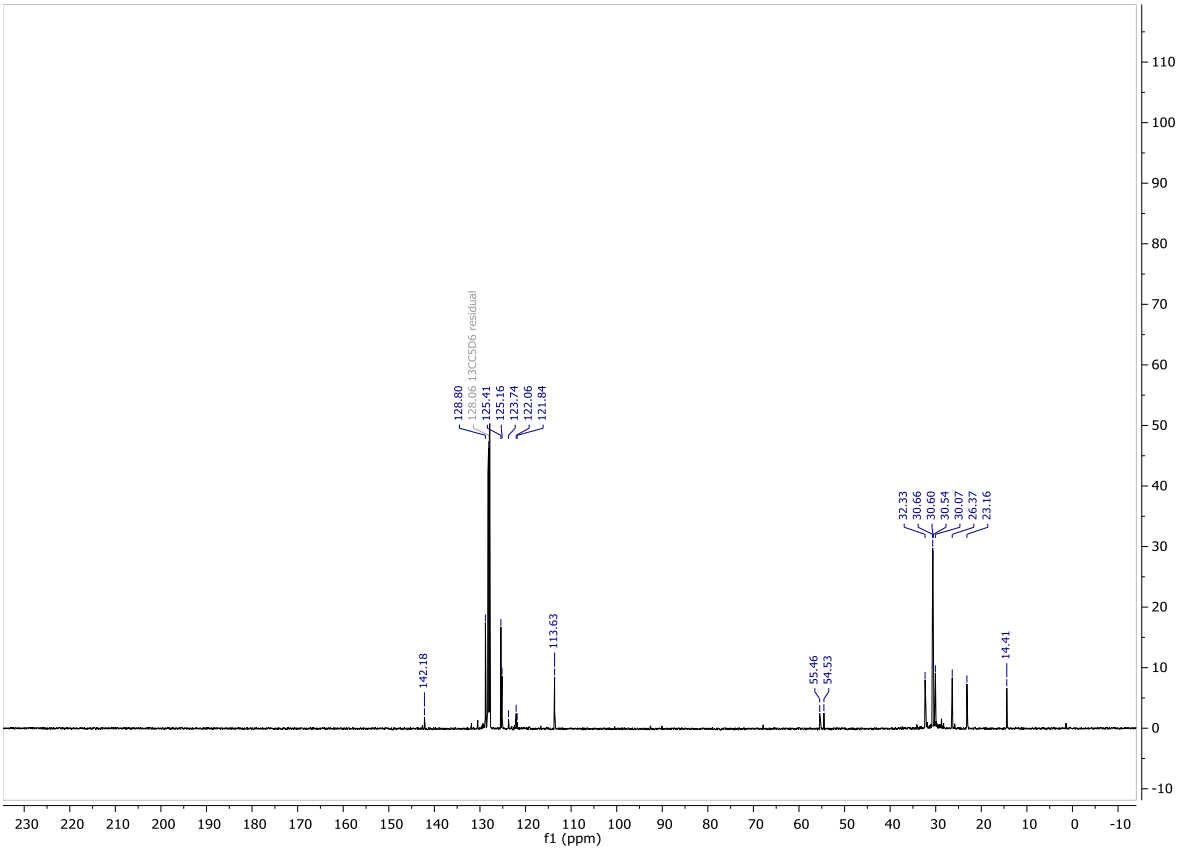

GCMS of the 4CC product and MS fragmentation pattern

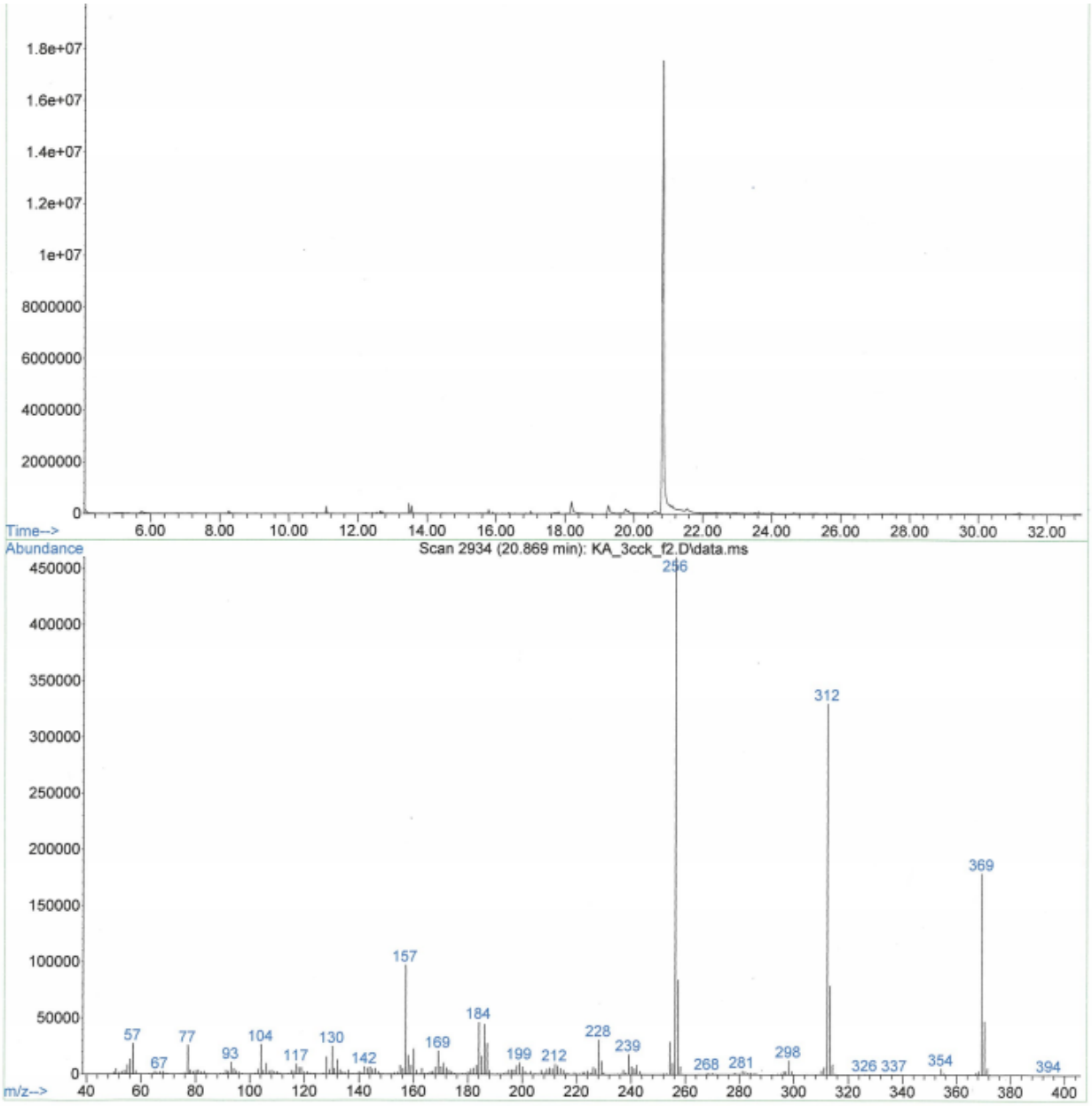

gCOSY NMR of the 4CC product in $CDCl_3$

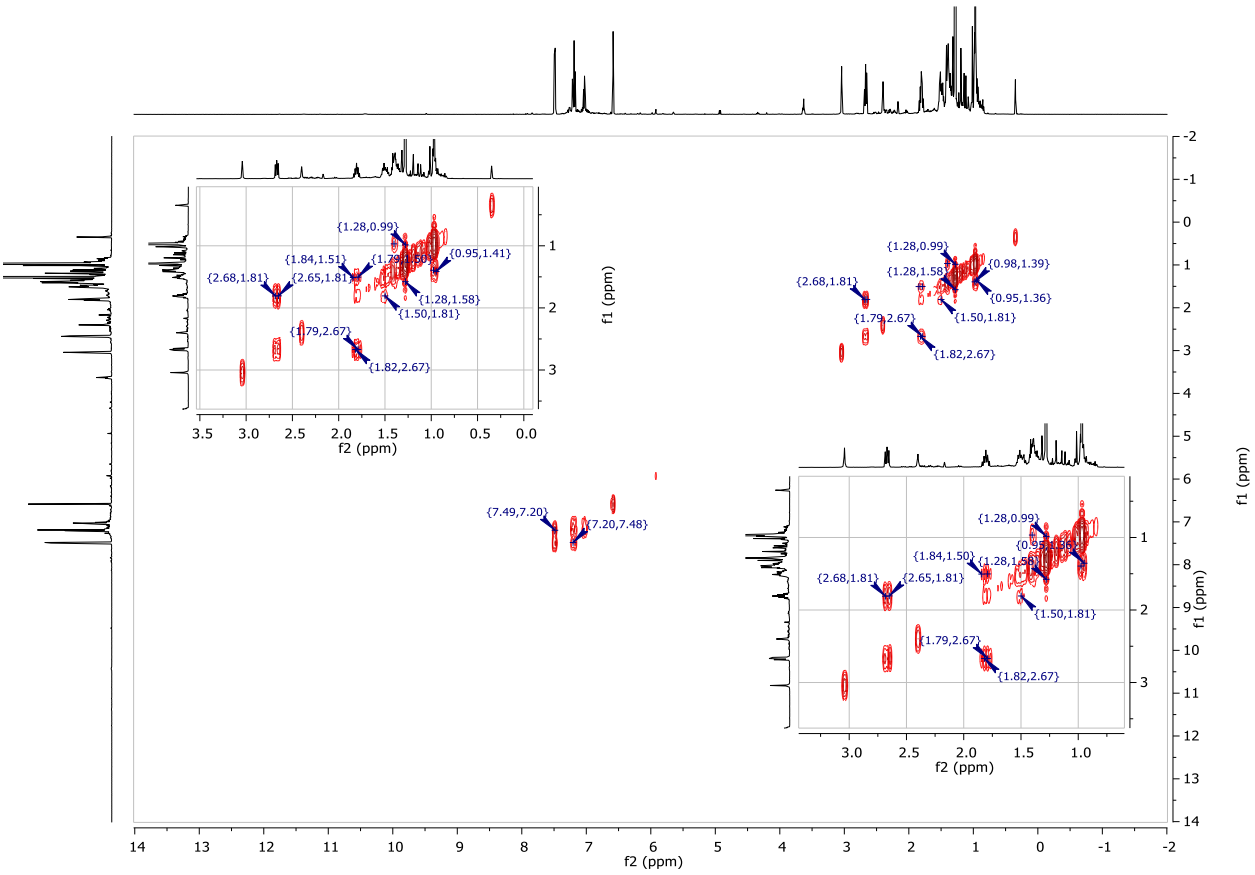

HMBC NMR of 4CC in $CDCl_3$

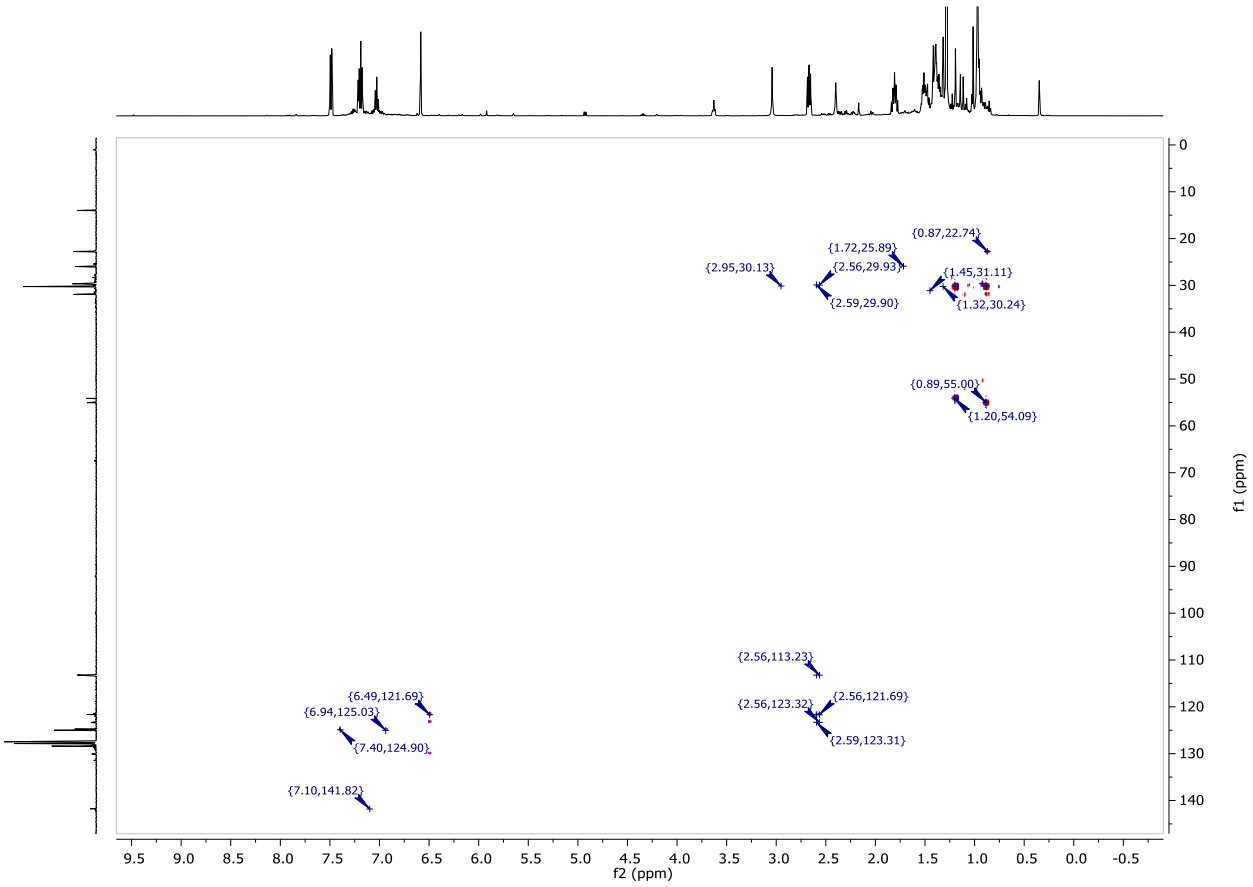

^{1}H NMR of $NCr(N^{i}Pr_2)_2(OPh^{4\text{-}methyl})$ in $CDCl_3$ at –27 °C

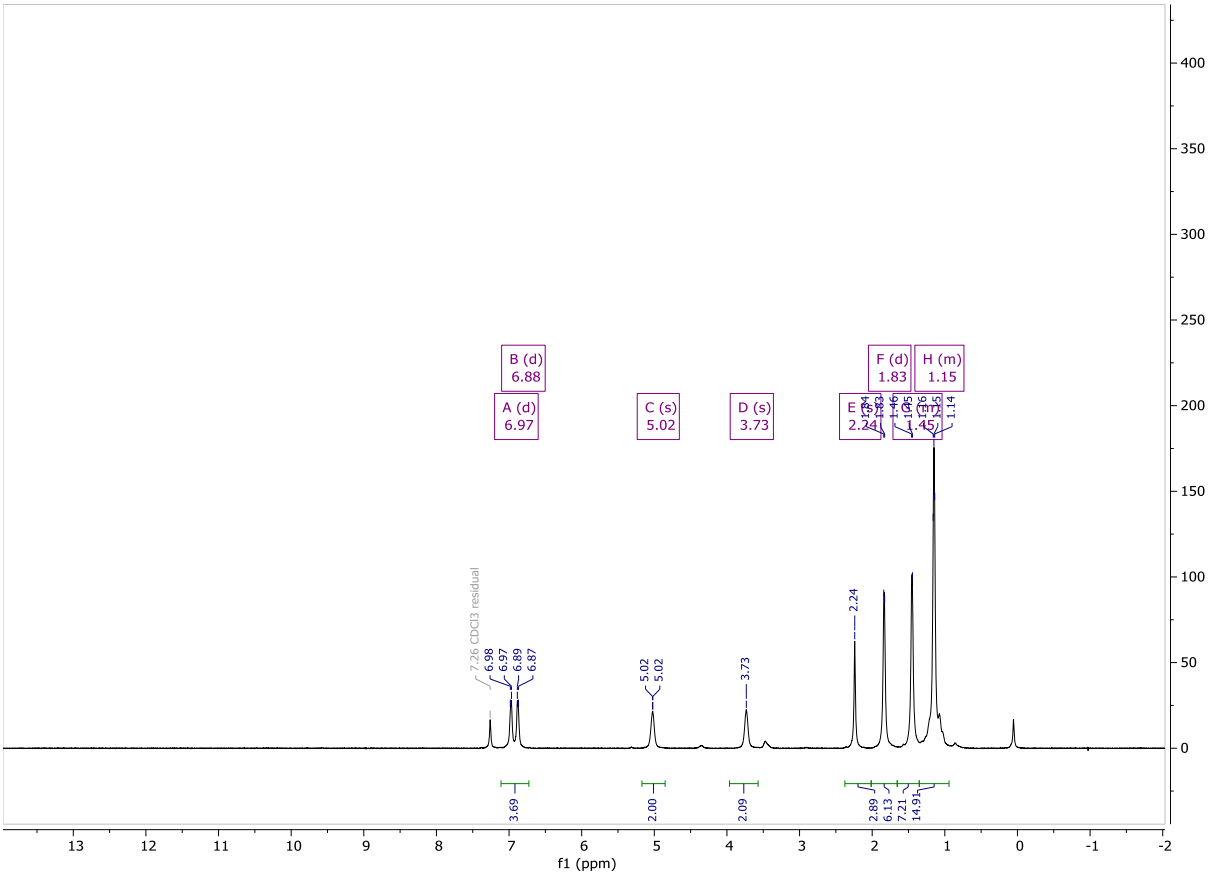

^{13}C NMR of $NCr(N^iPr_2)_2(OPh^{4\text{-methyl}})$ in $CDCl_3$ at –27 °C

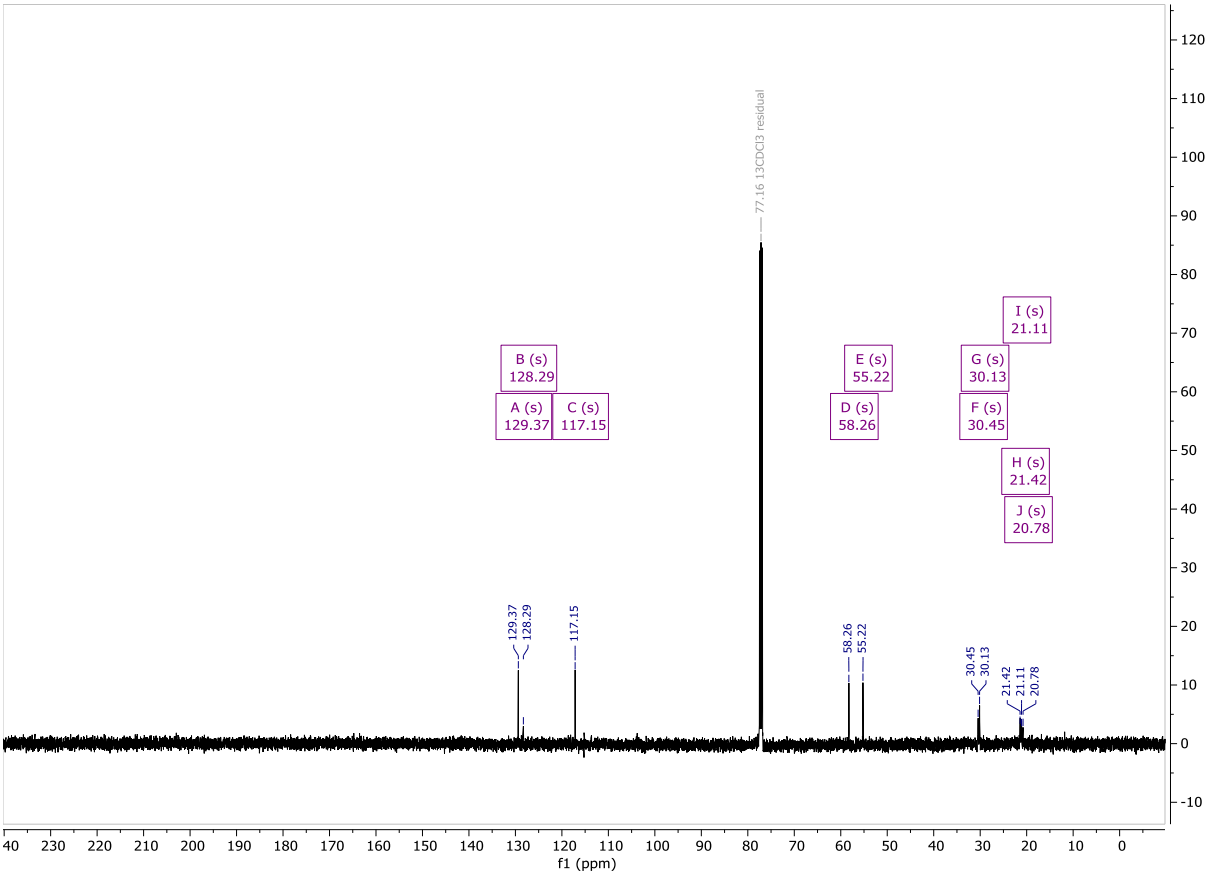

^{1}H NMR of $NCr(N^{i}Pr_2)_2(OPh^{4\text{-}bromo})$ in $CDCl_3$ at –20 °C

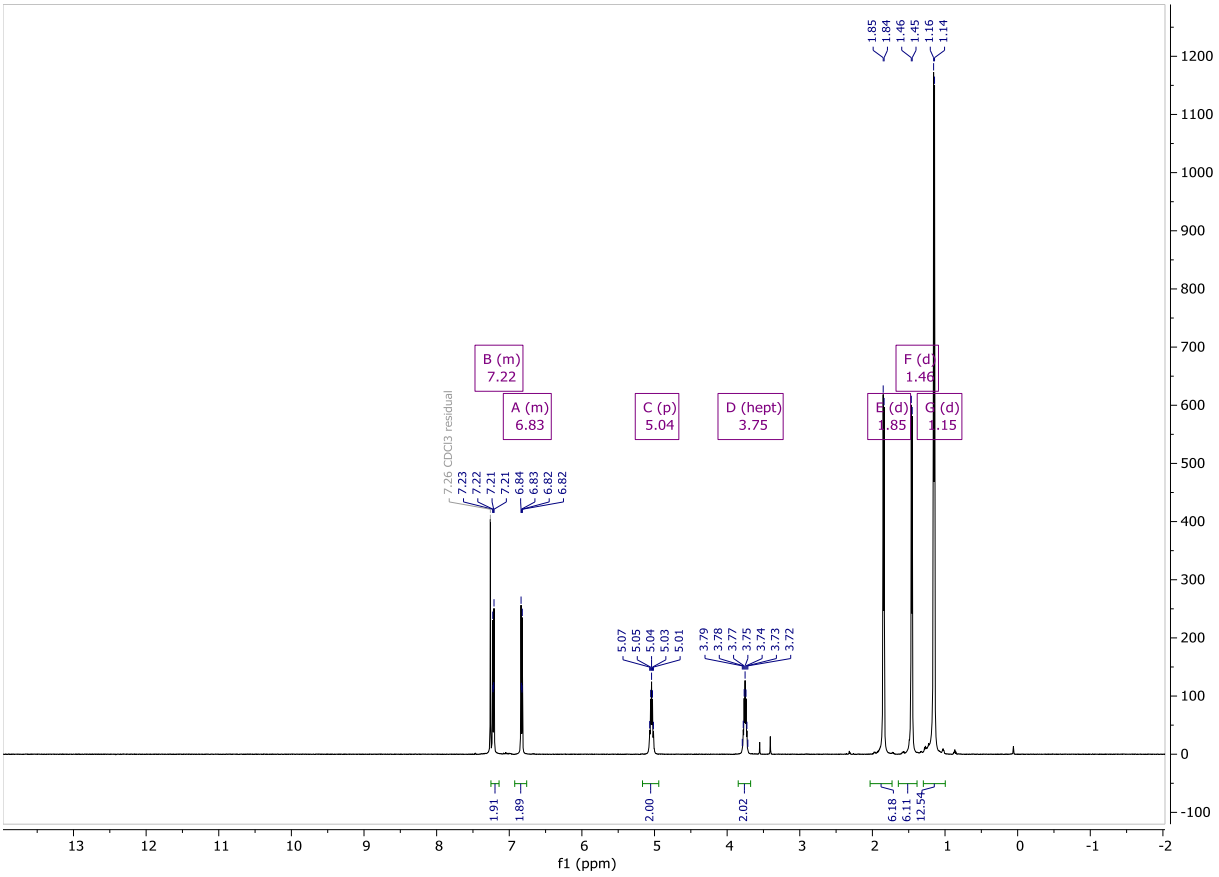

^{13}C NMR of $NCr(N^iPr_2)_2(OPh^{4\text{-}bromo})$ in $CDCl_3$ at –20 °C

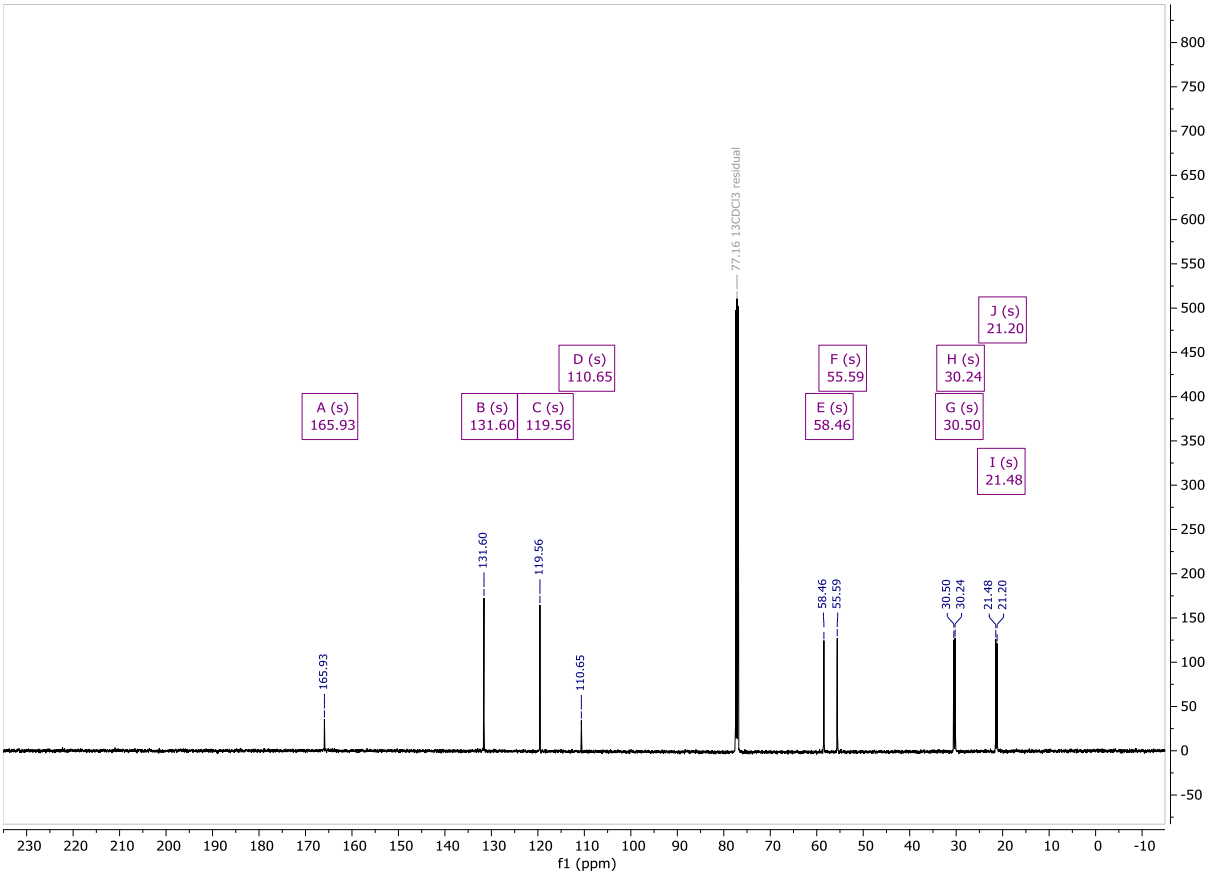

References

1. S. A. DiFranco, N. A. Maciulis, R. J. Staples, R. J. Batrice and A. L. Odom, *Inorg. Chem.*, 2012, **51**, 1187-1200.
2. E. Barnea, S. Majumder, R. J. Staples and A. L. Odom, *Organometallics*, 2009, **28**, 3876-3881.
3. S. A. DiFranco, N. A. Maciulis, R. J. Staples, R. J. Batrice and A. L. Odom, *Inorg. Chem.*, 2012, **51**, 1187-1200.
4. B. S. Billow, R. D. Bemowski, S. A. DiFranco, R. J. Staples and A. L. Odom, *Organometallics*, 2015, **34**, 4567-4573.
5. B. S. Billow, T. J. McDaniel and A. L. Odom, *Nature Chem.*, 2017, **9**, 837.
6. B. S. Billow, T. J. McDaniel and A. L. Odom, *Nature Chem.*, 2017, **9**, 837-842.
7. R. Carlson, Carlson J. E., *Design and Optimization in Organic Synthesis*, Elsevier, Amsterdam, 2nd edn., 2005.